Environmental Science & Technology

pubs.acs.org/est

Article

Isotopically Modified Bioassay Bridges the Bioavailability and Toxicity Risk Assessment of Metals in Bedded Sediments

Qiuling Wu, Qijing Su, Stuart L. Simpson, Qiao-Guo Tan, Rong Chen, and Minwei Xie*

Cite This: https://doi.org/10.1021/acs.est.2c06193

Read Online

ACCESS | Metrics & More | Article Recommendations | Supporting Information

ABSTRACT: The application of bioavailability-based risk assessment for the management of contaminated sediments requires new techniques to rapidly and accurately determine metal bioavailability. Here, we designed a multimetal isotopically modified bioassay to directly measure the bioavailability of different metals by tracing the change in their isotopic composition within organisms following sediment exposure. With a 24 h sediment exposure, the bioassay sensed significant bioavailability of nickel and lead within the sediment and determined that cadmium and copper exhibited low bioavailable concentrations and risk profiles. We further tested whether the metal bioavailability sensed by this new bioassay would predict the toxicity risk of metals by examining the relationship between metal bioavailability and metal toxicity to chironomid larvae emergence. A strong dose−toxicity relationship between nickel bioavailability (nickel assimilation rate) and toxicity (22 days emergence ratio) indicated exposure to bioavailable nickel in the sediment induced toxic effects to the chironomids. Overall, our study demonstrated that the isotopically modified bioassay successfully determined metal bioavailability in sediments within a relatively short period of exposure. Because of its speed of measurement, it may be used at the initial screening stage to rapidly diagnose the bioavailable contamination status of a site.

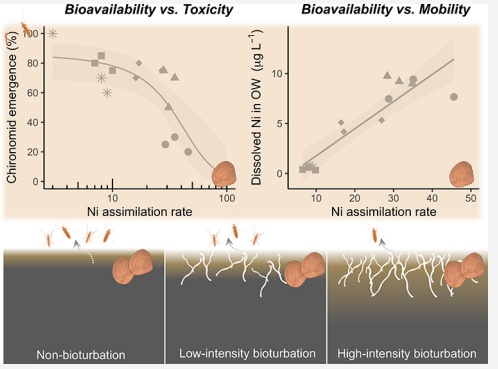

KEYWORDS: *metal bioaccumulation, metal stable isotope, nickel bioavailability, metal mobility, sediment quality risk assessment*

1. INTRODUCTION

Bedded sediments are considered the primary sink for metal contaminants in aquatic ecosystems and are also an important source for metal contaminants to transmit into the overlying water and through the food web.[1] The metal concentrations and forms (speciation) in the sediments influence the fraction of metals that may enter a biological entity (i.e., the bioavailable fraction) and pose a risk of causing adverse effects to the ecosystem.[2−4] Thus, bioavailability-based methods are expected to provide superior outcomes for sediment quality risk assessment, but the application of this concept has been greatly hampered by the inability of the current techniques to accurately and rapidly determine metal bioavailability in the sediments.[5−7]

The conventional approaches to directly assess metal bioavailability in sediments have relied heavily upon long-term bioaccumulation[4,8] and toxicity tests.[1,9,10] The former approach intends to quantify the bioavailability by comparing the tissue metal concentrations before and after the sediment exposure, while the latter approach indirectly derives the bioavailability relying on the metal exposure−toxicity relationship. Both approaches require long-term contaminant exposure to accumulate detectable and reliable changes in metal concentrations or for the toxic effects to manifest and are also challenged by the ability to replicate field conditions.[11,12]

The lack of efficiency of existing methods for assessing metal bioavailability hampers the broad application of bioavailability-based risk assessment for management of contaminated sediment sites, and new techniques to rapidly and accurately determine the metal bioavailability are in demand. The speciation and behavior of metals in the sediments are controlled by complicated and variable geochemical reactions.[1,2,13−15] Perturbations such as bioturbation or bioirrigation further modify the fate of metals in the sediments by translocating sediment particles and by changing the geochemical conditions.[16−18] The highly variable behavior of different organisms is also a necessary consideration when assessing bioavailability and toxicity risk of metals in sediments.[19] Consequently, new techniques should seek to incorporate organism behaviors that naturally influence the bioavailability and toxicity risk of sedimentary metals in natural settings and also minimize artifacts caused by excessive

Received: August 26, 2022
Revised: October 19, 2022
Accepted: November 2, 2022
Published: November 14, 2022

disturbance (e.g., homogenizing, sieving, and spiked-sediment equilibration) prior to method application.

Recently, Croteau et al. proposed a novel reverse-labeling approach to determine the bioavailability of copper[20] and zinc[21] individually on natural particles in waters. We subsequently adapted that core idea and substantially simplified the calculation to study the effects of sediment resuspension on the bioavailability of particulate metals (Cu, Zn, Cd) in suspended particles.[22] In those studies, the organisms were first prelabeled with metal stable isotopes to enrich the abundance of specific isotopes in the organism, and then these isotopically modified organisms were exposed to sediment particles to assess the portion of bioavailable metals. Because the sediment metals have a natural isotope composition that is different from the isotope composition in the organisms, the change in metal isotope composition within the organism due to the sediment exposure, brought about by assimilation of bioavailable metals, provided a measure of the bioavailability of metals associated with the sediment particles.

This study substantially extends the application of the isotopically modified bioassay to directly measure metal bioavailability in bedded sediments. The primary objective was to test whether the metal bioavailability sensed by this new bioassay would predict the toxicity risk of metals. The natural sediments with a different contamination status and modified densities of tubificid worms were used to create varying concentrations of bioavailable metals, and the release of metals to the overlying water and the toxicity of metals in the sediments were determined concurrently to evaluate their relationship with the measured metal bioavailability.

2. MATERIALS AND METHODS

2.1. Water, Sediment, and Organisms. A reconstituted freshwater was used to culture the clams and worms and for experiments and was prepared by dissolving 61.5 mg of $MgSO_4{\cdot}7H_2O$, 63.25 mg of $CaSO_4{\cdot}2H_2O$, 96 mg of $NaHCO_3$, 50 mg of $CaCl_2$, and 4 mg of KCl in every liter of deionized water.[23] The reconstituted freshwater was then gently aerated overnight before use.

Six metal stable isotopes with different purities (98.7% of ^{112}Cd, 99.07% of ^{114}Cd, 99.3% of ^{61}Ni, 99.36% of ^{62}Ni, 99.51% of ^{206}Pb, and 99.6% of ^{65}Cu) were purchased from ISOFLEX USA.

Sediments were collected in October 2021 from two sites: a clean site and a contaminated site. The relatively clean site was located in a headwater stream in a park of Shenzhen, China (22°33′49″ N, 113°57′10″ E), with low−moderate lead and zinc contamination. The contaminated site was located in a tributary river of the Pearl River Estuary in China (22°45′2″ N, 113°46′10″ E) where the sediment was heavily contaminated by multiple metals (Table S1, Supporting Information).[24−26] The sediments from both sites were fine-grained (Table S1) and anoxic (dark color with sulfide smell). Surficial sediments (<10 cm) were shoveled into plastic buckets, sealed, and transported back to the laboratory, where they were stored at room temperature (21 ± 1 °C).

Native organisms (oligochaete worms unidentified) present in the sediments were killed before sediments were used in the experiment. This was done by incubating the collected sediments underlying deoxygenated water,[27] which was continuously bubbled with the nitrogen gas at a rate of 40 mL min^{-1} for 2 weeks.

Three types of benthic organisms were used in this study. An Asian clam species (*Corbicula fluminea*), which can filter-feed on suspended particles and pedal-feed on sediment particles while buried in the sediments,[28] was the isotopically modified bioassay species. This species is widely distributed worldwide and has been suggested as a biological monitor in freshwater environments.[29] Tubificid oligochaete worms (*Limnodrilus hoffmeistteri*), which are deposit feeders that ingest sediments at depth and egest them at the sediment−water interface (SWI),[30] were used to modify the level of bioturbation in test treatments. These worms also tolerate high levels of contamination and are often the dominant species in highly contaminated freshwater sediments.[31] Chironomid larvae development is a commonly used toxicity assessment endpoint because these organisms develop rapidly to emerge as midges,[32] and *Chironomus kiiensis* was used here to assess sediment toxicity.

Clams, with a shell length of 1.6 to 2.2 cm, were collected at an uncontaminated stream (23°28′40″ N, 113°49′46″ E) in Guangdong Province, China, and shipped overnight to the laboratory. The clams were then acclimated in the reconstituted freshwater in laboratory conditions (21 ± 1 °C, 14 h: 10 h of light/dark cycle) for at least a week before being used in the experiment, during which they were fed the green algae *Chlorella* sp. (3.5 mg $clam^{-1}$) daily. Tubificid oligochaete worms (*Limnodrilus hoffmeistteri*, ca. 3 cm long, 1 mm in diameter), were purchased from a local aquarium culture. Chironomid larvae (*Chironomus kiiensis*) were obtained from laboratory cultures. Both the tubificid worms and chironomids were fed crushed fish food (c.a. 2 mg $individual^{-1}$, BFB-Made, Guangdong, China) three times a week.

2.2. Test Microcosms. Before each experiment, all plastic parts of the experimental system were soaked in 5% HNO_3 at least overnight and then thoroughly rinsed using deionized water (18.2 MΩ·cm).

Small microcosms were used to conduct the experiments, comprising a cuboid chamber and a water-circulation system. The chamber was made of transparent acrylic plastic and had dimensions of 15 cm (length) × 15 cm (width) × 30 cm (depth) (Figure S1, Supporting Information). It contained a 6 cm depth of the homogenized sediments (volume = 1.35 L), 15 cm depth of overlying freshwater (volume = 3.375 L), and a 9 cm depth of headspace (2.025 L) into which the chironomid midges could emerge. To retain the emerged midges and also to minimize water evaporation, each chamber was covered by a plastic sheet with drilled holes for water circulation (Figure S1b). The overlying water was constantly circulated within the closed system, passing through a chromatography column (27 mL volume, 2.2 cm inner diameter, and 7.1 cm length) containing a metal-binding resin (10 g of calcium-form[33] Chelex-100 resin, 100−200 mesh, Bio Rad, USA, 5 cm bed height) at a rate of 4.7 mL min^{-1} (corresponding to an overlying water turnover time of 0.5 day). To prevent suspended sediment entering the circulation system and clogging the resin column, a filtration unit comprising microporous hollow fibers (48 cm long, 2 mm in diameter, 0.15 μm pore size) was installed at the inlet of the circulation system (Figure S1). This water circulation system removed dissolved metals from the overlying water over the course of the experiment, with the intent of decreasing the concentrations of bioavailable metals in the overlying water (where in a natural environment this process may occur through dilution

https://doi.org/10.1021/acs.est.2c06193
Environ. Sci. Technol. XXXX, XXX, XXX−XXX

in an open system). The water flowing out of the chromatography column was then discharged back to the overlying water at the top of the chamber. The overlying water was continuously oxygenated by a gentle stream of air through an aquarium stone, at a height that provided water mixing without suspending the sediments.

2.3. Experimental Procedure. To each of the 15 chambers, homogenized sediments devoid of organisms were carefully added to form a 5 cm-deep sediment bed with a flat surface. To enable time-series porewater sampling, two self-assembled microporous porewater samplers (5 cm long, 2 mm in diameter, pore size of 0.15 μm, polyvinylidene fluoride material, Wanxi Environmental Science and Technology Co., LTD, Shandong, China) (Figure S1c,d) were inserted through predrilled holes on the side wall of the chambers at depths of 1 and 3 cm below the SWI. Freshwater was then slowly added into the chamber to form a 15 cm-deep overlying water column. The sediment−water system was stabilized for 24 h for the sediment to consolidate. The overlying water was then renewed, and the 22 day experiment commenced by introducing the tubificid worms and chironomid larvae into the system.

Different densities of tubificid worms were added to tests to enable changes of metal bioavailability. Tubificid worms were evenly distributed at the sediment surface in treatments with bioturbation, and these worms immediately burrowed into the sediments within 30 min. There were three contaminated sediment treatments amended with no worms, ca. 200 worms (0.307 g wet weight of worms) and ca. 400 worms (0.614 g wet weight of worms), corresponding to a nominal average density of 0, 10,000 and 20,000 individuals m^{-2}, respectively, and these conditions were denoted as the no-worm (Cont-NW), low-density (Cont-LD), and high-density (Cont-HD) conditions. Because the 5 cm sediment depth and the chamber walls may slightly restrict the activity of worms, the experimental conditions used a slightly lower worm density range (0 to 20,000 individuals m^{-2}) than the one that occurs naturally (the natural density of tubificid worms varies with orders of magnitude difference, with a density reaching as high as 10^5 individuals m^{-2}).[30,34−36] There were two clean sediment treatments with no worm (Ref-NW) and the high-density of worms (Ref-HD). Each treatment condition was tested in triplicate.

Once the added tubificid worms had buried, 20 chironomid larvae (first instar) were then added into each chamber to determine the toxicity of sediments (Section 2.5). On Day 20, the overlying water in the chamber was drained to about 1 cm depth and then 10 isotopically modified clams (Section 2.4) were added into each chamber (evenly distributed at the sediment surface). The chambers were then refilled to the original depth with new freshwater, and the experiments continued for a further 24 h. The experiments were terminated on day 21, the overlying water was drained, and the clams were recovered for analysis.

2.4. Bioavailability Determination Using the Isotopically Modified Bioassay. The bioavailability of metals in sediments was directly quantified using a multimetal isotopically modified bioassay technique developed in our previous study.[22] The metal bioavailability was determined by tracing the change of metal isotopic composition in clam tissue following sediment exposure. This method involved three stages: isotope-enriching in clam tissue, sediment exposure to clams, and depuration of clams to clear undigested sediments.

Before being exposed to sediments, the clams were cultured in 10 L of metal isotope-spiked freshwater for 10 days to enrich the labeling isotopes in their tissue. Six different metal isotopes (2 $\mu g\ L^{-1}$ ^{112}Cd, 3 $\mu g\ L^{-1}$ ^{114}Cd, 5 $\mu g\ L^{-1}$ ^{61}Ni, 5 $\mu g\ L^{-1}$ ^{62}Ni, 5 $\mu g\ L^{-1}$ ^{206}Pb, and 10 $\mu g\ L^{-1}$ ^{65}Cu) were added into the reconstituted freshwater prior to the experiment. To maintain constant concentrations of these metal isotopes during the enriching stage, a flow-through aqueous isotopic enriching system was used and the isotope-spiked freshwater was renewed at a rate of 10.5 mL min^{-1}. During the isotope-enriching stage, the clams were fed the green algae (3.5 mg $clam^{-1}$) daily in separate containers. The suspension feeding lasted 1 h, and the clams were thoroughly rinsed with clean freshwater before they were returned to the flow-through system. Ten clams were sampled on each of days 0, 3, and 10 before feeding to monitor the isotopic composition in their tissue. After removal from the solution, these clams were immediately immersed into 1 mM EDTA solution for 1 min to terminate metal isotope uptake and then dissected using a stainless-steel scalpel. Their soft tissue was removed from the clam shell, rinsed with the EDTA solution and then deionized water twice, and stored in a −20 °C refrigerator before metal analysis.

On day 20 of the experiment (immediately after the water change), 10 isotopically modified clams were spread on the surface of each sediment treatment and all buried within 30 min. Following a 24 h sediment exposure, these clams were retrieved, washed with reverse-osmosis water to clear attached particles, and then placed in clean reconstituted freshwater (1 L) to depurate for 8 h (not fed during this period). The water was renewed once when fecal matter was observed at the bottom of the depuration container (after ca. 4 h), to minimize metal assimilation from the feces. At the end of depuration, the clams were rinsed using deionized water and dissected as described above and their soft tissue was frozen stored for further treatment.

A separate group of isotopically modified organisms (denoted as the baseline treatment) were processed in the same way but were not exposed to the sediments. Instead, they were placed in clean freshwater for 24 h and then subjected to the same depuration and dissection procedures. The isotopic composition in these clams provided as a baseline as the isotopically modified clams were not exposed to bioavailable metals. Therefore, a decrease of the isotopic composition from the baseline composition in the clams following sediment exposure would signal the assimilation of bioavailable metals.

2.5. Toxicity Test with Chironomid Larvae. Sediment toxicity was assessed by determining adverse effects to the chironomid emergence process (time and rate) following the standard protocols with minor modifications.[32,37,38] Briefly, 20 first-instar chironomid larvae (5 days after hatching) were added into the sediments on day 0 and their emergence process was monitored over the course of the experiment. They were fed daily by adding crushed fish food directly into the chamber (20 mg day^{-1} for days 1−10 and then 40 mg day^{-1} for days 11−21). The first emergence of chironomid midge was observed on day 13, and the emergence was then recorded daily. The emerged midges were subsequently removed from the chamber. The (cumulative) emergence ratio (the number of emerged chironomids:total number of chironomids added, %) was calculated and used as a sublethal toxicity endpoint.

https://doi.org/10.1021/acs.est.2c06193
Environ. Sci. Technol. XXXX, XXX, XXX−XXX

2.6. Sampling and Analysis. The sediments were initially characterized for total recoverable metal (TRM) concentrations and particle size distribution (Note S1 and Table S1, Supporting Information).

During the experiment, the pH and dissolved oxygen (DO) concentrations in the overlying water of each chamber was monitored (Note S1, Supporting Information). Five milliliters of overlying water was sampled daily for measurement of dissolved metal concentrations. The water was filtered (PES membrane filter with 0.45 μm pore size), acidified with concentrated nitric acid (70%, trace metal grade, Sigma-Aldrich) to a pH of <2, and stored at 4 °C until analysis. Following the overlying water sampling, 5 mL of clean reconstituted water was added into each chamber to compensate the sampling loss.

Porewater samples were extracted via the subsurface microporous samplers (with a pore size of 0.15 μm,) at 1 and 3 cm below the SWI on days 0, 4, 8, 12, 16, and 21. The first 0.5 mL of porewater was discarded, and then another 2 mL of porewater was collected, acidified to a pH < 2, and stored for metal concentration analysis.

Metal concentrations (Cd, Cu, Ni, and Pb) in the overlying water, porewater, and sediment digest solution were determined by the ICP-MS (inductively coupled plasma mass spectrometry, PerkinElmer NexION 2000). Metal isotope concentrations (^{111}Cd, ^{112}Cd, ^{114}Cd, ^{60}Ni, ^{61}Ni, ^{62}Ni, ^{206}Pb, ^{207}Pb, ^{63}Cu, and ^{65}Cu) in the clam tissue digest solution were also determined by the ICP-MS. A series of quality control procedures were also included, as detailed in the Supporting Information (Note S1 and Table S2, Supporting Information).

The clam tissue samples were freeze-dried and then digested in 0.5 mL of 65% HNO_3 at 80 °C for 8 h. Concurrently, a certified reference material (oyster tissue, SRM 1566b) was also digested following the same method (and the recovery was reported in Table S2). These acid digests were diluted and metal concentrations analyzed by ICP-MS.

2.7. Data Analysis. The aqueous uptake of metal stable isotopes during the isotope-enriching stage, the isotopic ratios (labeled:unlabeled isotopes) in the clam tissue, and the metal assimilation rate from the sediments (i.e., metal bioavailability) can be quantified by tracing the change in the isotopic composition of the clam tissue at the end of different stages, as detailed in the Supporting Information. As an example, we provide details of the data analysis of Ni^{61}, while the equations for other metals are provided in the Supporting Information (Note S2, Supporting Information).

2.7.1. Aqueous Uptake of Ni^{61} during the Isotope-Enriching Stage. During the isotope-enriching stage, the clam tissue concentration of the labeling isotope Ni^{61} increases, while that of the unlabeled isotope Ni^{60} remains unchanged (p = 0.754, Student's t-test). The total tissue concentration of Ni^{61} ($[^{61}Ni]_{tot}$) consists of the background tissue concentration of Ni^{61} ($[^{61}Ni]_{bkg}$, can be derived from the concentration of Ni^{60}) and the newly accumulated tissue concentration of Ni^{61} ($[^{61}Ni]_{new}$, μg g^{-1} dry weight). The $[^{61}Ni]_{new}$ thus can be calculated as the difference between the $[^{61}Ni]_{tot}$ and the $[^{61}Ni]_{bkg}$ (the derivation is illustrated in Figure S2, Supporting Information).[39] Both the $[^{61}Ni]_{tot}$ and $[^{61}Ni]_{bkg}$ were determined by measuring the isotope concentration of ^{61}Ni and ^{60}Ni in a tissue sample from the same organism.

$$[^{61}Ni]_{new} = [^{61}Ni]_{tot} - [^{61}Ni]_{bkg} \quad (1)$$

$$[^{61}Ni]_{tot} = [^{61}Ni]_{meas} \times 1.14\% \quad (2)$$

$$[^{61}Ni]_{bkg} = [^{60}Ni]_{meas} \times 1.14\% \quad (3)$$

where $[^{61}Ni]_{meas}$ and $[^{60}Ni]_{meas}$ (μg g^{-1}) are the total tissue concentrations of Ni derived from total Ni concentrations (μg L^{-1}) reported by measuring the signal of ^{61}Ni and ^{60}Ni and assuming the nickel in the sample has a natural isotopic composition. Theoretically, in an unlabeled organism, these two concentrations ($[^{61}Ni]_{meas}$ and $[^{60}Ni]_{meas}$) are the same (ignoring the subtle difference induced by isotope fractionation); because the ^{61}Ni is enriching in the organism, $[^{61}Ni]_{meas}$ and $[^{60}Ni]_{meas}$ become different. The number 1.14% is the natural isotope abundance of ^{61}Ni (Table S3, Supporting Information).

The isotopic ratio between the labeled and unlabeled isotope ($Ni^{61/60}$) was calculated as follows:

$$Ni^{61/60} = \frac{[^{61}Ni]_{meas} \times 1.14\%}{[^{60}Ni]_{meas} \times 26.2\%} \quad (4)$$

where the number 26.2% is the natural isotope abundance of ^{60}Ni. In an unlabeled organism, because $[^{61}Ni]_{meas}$ and $[^{60}Ni]_{meas}$ are the same, the $Ni^{61/60}$ equals 0.043.

Therefore, the isotopic ratio of the clams in the baseline treatment (isotopically modified clams without sediment exposure) $Ni^{61/60}|_{base}$ and that of the clams in the treatment with sediment exposure $Ni^{61/60}|_{exp}$ were calculated in eqs 5 and 6, respectively.

$$Ni^{61/60}|_{base} = \frac{[^{61}Ni]_{meas|base} \times 1.14\%}{[^{60}Ni]_{meas|base} \times 26.2\%} \quad (5)$$

$$Ni^{61/60}|_{exp} = \frac{[^{61}Ni]_{meas|exp} \times 1.14\%}{[^{60}Ni]_{meas|exp} \times 26.2\%} \quad (6)$$

where $[^{61}Ni]_{meas|base}$, $[^{60}Ni]_{meas|base}$, $[^{61}Ni]_{meas|exp}$, and $[^{60}Ni]_{meas|exp}$ (μg g^{-1}) are the total tissue concentrations of nickel reported by measuring the concentration of ^{61}Ni and ^{60}Ni in the baseline treatment and the sediment-exposure treatment.

2.7.2. Metal Assimilation Rate from the Bedded Sediment. When the isotopically modified clams assimilate Ni from the sediment, the isotopic ratio $Ni^{61/60}$ decreases. The Ni assimilation rate (μg g^{-1} h^{-1}) can be derived by calculating the assimilation mass of Ni (M_{Ni}, μg) that causes the decrease of the isotopic ratio from $Ni^{61/60}|_{base}$ to $Ni^{61/60}|_{exp}$ (eqs 7 to 9).

$$Ni^{61/60}|_{base} = \frac{W \times [^{61}Ni]_{meas|exp} \times 1.14\% - M_{Ni} \times 1.14\%}{W \times [^{60}Ni]_{meas|exp} \times 26.2\% - M_{Ni} \times 26.2\%} \quad (7)$$

$$M_{Ni} = W \times (Ni^{61/60}|_{base} \times [^{60}Ni]_{meas|exp} \times 26.2\% - [^{61}Ni]_{meas|exp} \times 1.14\%)/(Ni^{61/60}|_{base} \times 26.2\% - 1.14\%) \quad (8)$$

$$\text{assimilation rate of Ni} = \frac{M_{Ni}}{W \times t_{exp}} \quad (9)$$

where W is the dry weight of the clam tissue and t_{exp} is the sediment exposure time (here, it is 24 h).

https://doi.org/10.1021/acs.est.2c06193
Environ. Sci. Technol. XXXX, XXX, XXX−XXX

3. RESULTS AND DISCUSSION

3.1. Metal Bioavailability Determined by the Isotopically Modified Bioassay. During the 10 day isotope-enriching stage, the clams steadily absorbed metal isotopes from the isotope-spiked water (Figure S3, Supporting Information). The uptake of the metal isotopes caused enrichment of these labeled isotopes in the clam tissue, and the extent of isotope enrichment (the abundance ratio between the labeled and unlabeled isotopes) differed among the metals. On day 10, the newly accumulated concentrations of ^{112}Cd, ^{114}Cd, ^{65}Cu, ^{206}Pb, ^{61}Ni, and ^{62}Ni in the clams increased from 0 to 3.4 ± 0.8, 4.8 ± 1.1, 17 ± 5, 2.0 ± 0.7, 0.75 ± 0.18, and 0.74 ± 0.18 μg g^{-1}, respectively. The increase in the isotopic ratios is a function of both the net uptake rate of metal isotopes from the water (proportionally) and the background tissue metal concentrations (inversely) (Table S4, Supporting Information). Here, the isotopic ratios in the clams increased from 1.8 to 28 ± 3.7 for $Cd^{112/111}$, from 2.2 to 39 ± 5 for $Cd^{114/111}$, from 0.44 to 1.2 ± 0.29 for $Cu^{65/63}$, from 1.1 to 80 ± 8 for $Pb^{206/207}$, from 0.046 to 12 ± 5 for $Ni^{61/60}$, and from 0.14 to 12 ± 5 for $Ni^{62/60}$ (Figure 1a,c,e,g,i,k).

Metal bioavailability in the bedded sediments was informed by the relative changes of isotopic ratios between the isotopically modified clams following sediment exposure and the isotopically modified clams in the baseline treatment without sediment exposure (Figure 1b,d,f,h,j,l). If no metals were assimilated by the clams, the isotopic ratios of the experimental groups would not be different from those of the reference group; otherwise, if bioavailable metals were assimilated, the isotopic ratios of the experimental groups would be lower than those of the reference group. Here, the isotopic ratios of cadmium and copper ($Cd^{112/111}$, $Cd^{114/111}$, and $Cu^{65/63}$) in clams exposed to different sediments remained the same as those in the baseline treatment (Figure 1b,d,f), suggesting that the bioavailability of cadmium and copper in the sediments was low. In contrast, the isotopic ratios of nickel and lead in the clams following sediment exposure were lower than those in the baseline treatment (Figure 1h, j, l), suggesting that the bioavailable concentrations of nickel and lead in the sediments were present. The $Ni^{61/60}$ and $Ni^{62/60}$ in the clams exposed to different sediments varied between 3.4 and 9.3 ($Ni^{61/60}|_{base}$ = $Ni^{62/60}|_{base}$ = 12 ± 1.5), while the $Pb^{206/207}$ varied between 19 and 43 ($Pb^{206/207}|_{base}$ = 69 ± 10) among different treatments, indicating that the bioavailability of these two metals differed among different sediments.

The decrease in the isotopic ratios of nickel and lead was converted to the average assimilation rates of these two metals over the course of 24 h sediment exposure (eqs 7 and 8) (Figure 2). The nickel assimilation rates ranged from 7.0 to 36 ng g^{-1} h^{-1} among different treatments. The assimilation rates calculated independently from the change of $Ni^{61/60}$ and $Ni^{62/60}$ were not significantly different, indicating consistent behavior of different metal isotopes during the implementation of this approach. The nickel assimilation rates were lower in the clean sediments relative to those in the contaminated sediments. In the treatment with contaminated sediments, the nickel assimilation rates increased with increasing density of the tubificid worms, suggesting that bioturbation by the tubificid worms increased nickel bioavailability in the contaminated sediments.

The lead assimilation rates were lower than the nickel assimilation rates, ranging from 2.1 to 3.8 ng g^{-1} h^{-1}. They were higher in the clean sediments than in the contaminated sediments, indicating the presence of more bioavailable lead in the clean sediments (consistent with that higher total concentrations of lead were in the clean sediments; Table S1). The lead assimilation rates were also higher in the treatments with higher density of worms (in both the clean and contaminated sediments) (Figure 2), suggesting that bioturbation by the tubificid worms also increased Pb bioavailability.

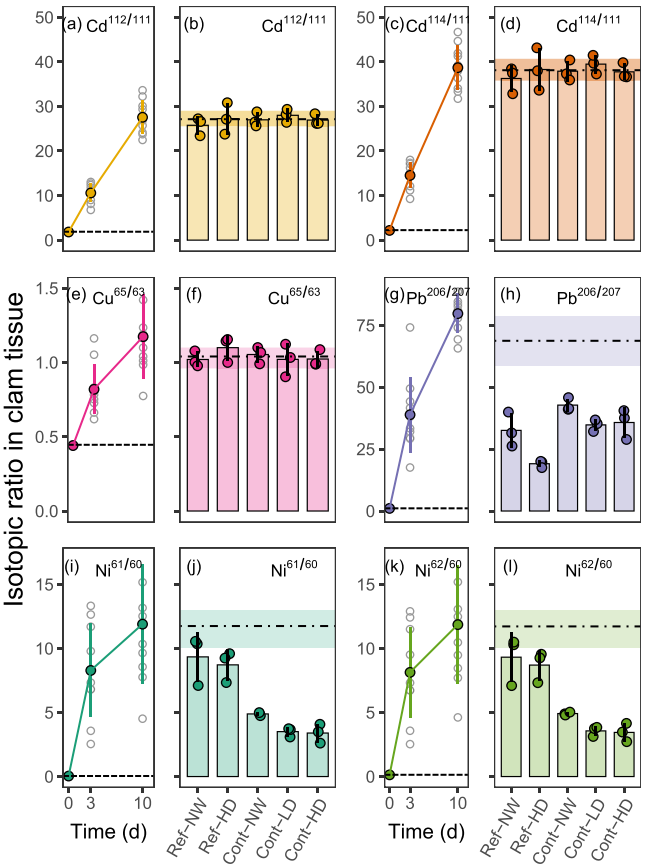

Figure 1. Change in the isotopic ratios of the clam tissue during the isotope-enriching stage and during the sediment exposure stage. (a, c, e, g, i, k) The isotopic ratio of different metals steadily increased during the isotope enriching stage. Each open circle represents the isotopic ratio of an individual clam. The solid point and the error bar represent the mean isotopic ratio and the standard deviation of the group. The dashed line represents the background isotopic ratio (natural isotope abundance) in unlabeled clams. (b, d, f, h, j, l) Variation of the isotopic ratio in the clam tissue following sediment exposure. The horizontal dot-dashed line (mean) and the band (standard deviation) represent the metal isotopic ratio of the clams in the baseline treatment that were not exposed to sediment. Each solid point represents the mean isotopic ratio of clams in a replicate treatment. The columns and the error bars represent the mean isotopic ratio and the standard deviation of the three replicates for each of the five sediment treatments.

3.2. Sediment Toxicity. Exposure to different sediments influenced the development of the chironomid larvae and their rate of emergence as chironomid midge (adults) (Figure 3). In the Ref-NW treatment, the chironomids started to emerge on day 13 and the emergence ratio gradually increased and approached to a constant ratio on day 17. The final emergence ratio (22 day emergence ratio) in this treatment was 80 ± 5%, which fulfills the requirement that the emergence ratio of the

https://doi.org/10.1021/acs.est.2c06193
Environ. Sci. Technol. XXXX, XXX, XXX−XXX

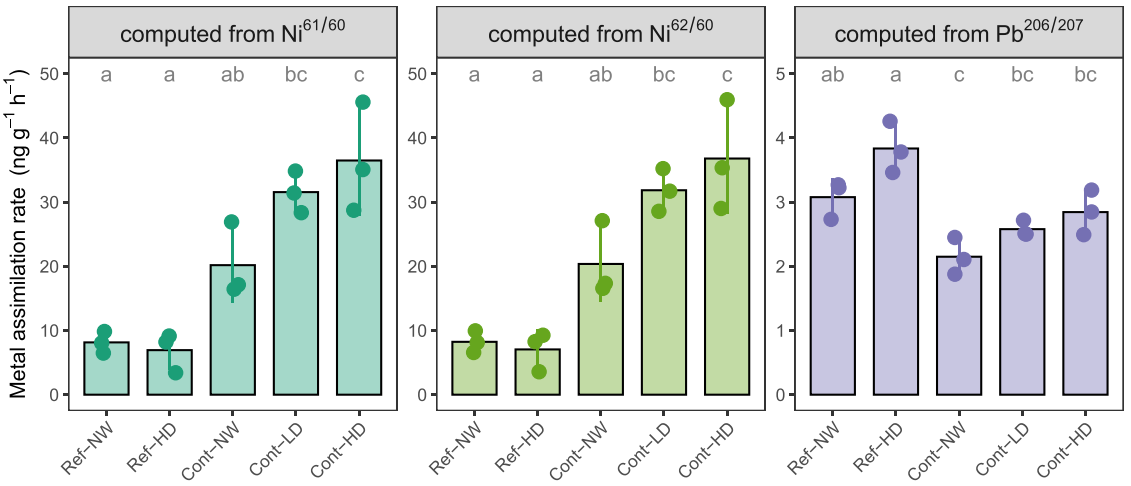

Figure 2. The metal assimilation rates varied among different sediments. Each solid point represents the mean assimilation rate in a replicate treatment. The column and the error bar represent the mean assimilation rate and the standard deviation of the three replicate treatments. The mean assimilation rates across different treatments sharing no common lower case letters were significantly different ($p < 0.05$).

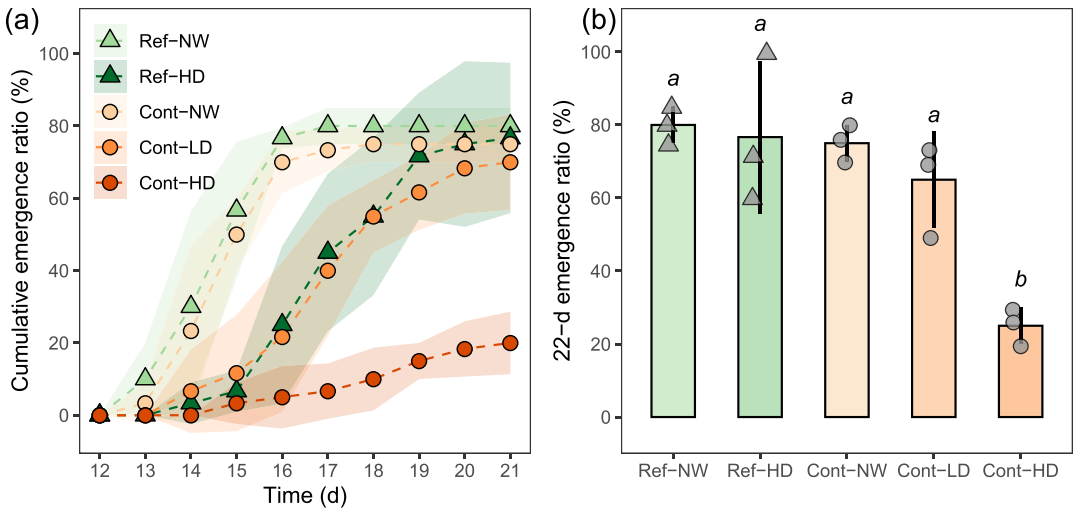

Figure 3. Emergence process of the chironomid midges exposed to different sediments. (a) Temporal change in the cumulative emergence ratio. The solid point represents the mean ratio of the three replicate treatments, and the shaded bands indicate the standard deviation of the mean. (b) 22 day emergence ratio of the chironomid midges in different sediments. Each gray solid point represents a measurement in a replicate treatment. The height of each column and the error bar represent the mean and the standard deviation of three replicates. The treatments sharing different letters were statistically different ($p < 0.05$).

chironomids in a reference sediment should be at least 70%.[32] The presence of tubificid worms delayed the emergence of the chironomids (Figure 3a). The chironomids in the Ref-HD sediment emerged on day 14, and the emergence ratio gradually approached to 76 ± 20% on day 21. This delay of the full development of the chironomids (through larvae stages to emerge as midges) was likely caused by the competition of tubificid worms for oxygen at the surficial sediments.

In sediments without tubificid worms (Ref-NW and Cont-NW), the chironomid worms were fully buried in the sediments throughout the experiment, whereas in the sediments with tubificid worms, we observed that the chironomid larvae extended into the water and swang their body to irrigate overlying water into the sediments. These behavioral differences were likely attributed to changes in the habitat within the sediments (Figure S4, Supporting Information) and potential competition between the tubificid worms and chironomid larvae for oxygen need. The presence of the tubificid worms (more tolerant to low-oxygen conditions[40]) may have consumed oxygen in the porewater, as an enhanced release of dissolved manganese was observed in treatments with increasing density of tubificid worms (Figure S5, Supporting Information). The consumption of oxygen in surficial porewater may thus result in the chironomid larvae needing to be closer to the SWI to fulfill their oxygen needs, and this likely reduces the energy allocation to their growth and may delay the development of chironomids.

Although the emergence process of the chironomids was delayed when the tubificid worms were present, the final emergence ratio of the chironomids at the end of the test was not influenced (Figure 3b). Therefore, the decrease in the final emergence ratio (22 day emergence ratio) was attributed to sediment toxicity. Here, exposure to contaminated sediments alone (Cont-NW) did not induce toxic effects on the emergence of chironomids (75 ± 13%, $p = 0.98$, one-way ANOVA followed by Turkey HSD test). However, sediment

https://doi.org/10.1021/acs.est.2c06193
Environ. Sci. Technol. XXXX, XXX, XXX−XXX

toxicity in the contaminated sediments was observed in the presence of bioturbating tubificid worms. The emergence ratio was 65 ± 13% in the contaminated sediment with a low density of tubificid worms (Cont-LD) (but not significantly different from that of the Con-NW, $p = 0.54$). The presence of a high density of worms significantly decreased the emergence ratio to 25 ± 5% ($p < 0.01$).

3.3. Relationship between Toxicity and Bioavailable Metal Exposure. The sublethal effects on chironomid larvae emergence was ascribed to exposure of bioavailable metals in the sediments. A strong metal exposure (dose)−toxicity relationship existed between the nickel assimilation rate and the 22 day emergence ratio of the chironomid larvae (Figure 4), suggesting that exposure to bioavailable nickel in the sediment induced toxic effects to the chironomids. In contrast, the lead assimilation rate did not adequately predict the biological response (Figure S6, Supporting Information), which was not surprising given the low lead assimilation rates.

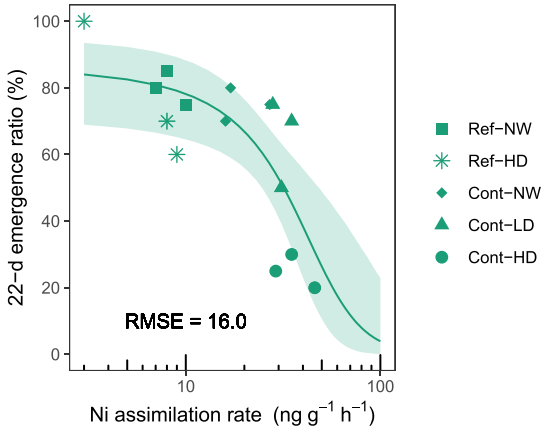

Figure 4. Sediment toxicity was well explained by exposure to bioavailable nickel in the sediments. Each point represents the measurement in a replicate test (five sediment treatments); the solid line is the regression line of the measurement using the logistic model, and the band is the 95% confidence band. RMSE stands for the root mean square error of the regression.

To further quantitatively assess the performance of using the nickel assimilation rate to predict sediment toxicity, we employed a logistic model to fit the data (Note S3, Supporting Information). While only five treatments were examined experimentally, the regression was applied to the results obtained from the 15 individual replicate experiments. The reason for treating each replicate experiment individually was because we expected the sediment heterogeneity to develop differently for each replicate during the test owing to differences in organism behavior. Although the sediments were initially homogenized in each treatment, the addition of bioturbating organisms (the exact number and the size of worms added could be different within the same treatment) and the behavioral difference of each individual organism over the 22 days can gradually create substantial physical and chemical heterogeneity in the sediment. Therefore, it was rational to fit the results of 15 individual replicate experiments, rather than fit the mean results of the 5 treatments.

The probability (p value) associated with the slope parameter of the logistic model was 0.0045 (Table S6), suggesting a significant dose−response relationship between the 22 day emergence ratio of the chironomids and the nickel assimilation rate by the clams (Figure 4; Note S3, Supporting Information).

The dose−toxicity relationship allows the calculation of thresholds for the sublethal effects as effect concentrations (EC). The calculated EC_{20} and EC_{50} for the 22 day emergence ratio were 8.7 and 32 ng g^{-1} h^{-1}, respectively. Thus, adverse effects on chironomid emergence may be expected when the nickel assimilation fluxes by the clams *Corbicula fluminea* exceed 8.7 ng g^{-1} h^{-1}.

3.4. Relationship between the Release of Metals into the Overlying Water and the Metal Bioavailability. The release of dissolved metals to the overlying water changed among different treatments and with different metals (Figure S5, Supporting Information). Dissolved metal concentrations were higher in treatments with more contaminated sediments (higher Ni, Cd, and Cu in Cont- treatment and higher lead in Ref- treatment). The presence of worm bioturbation enhanced the release of Ni, Pb, and Mn, although the difference for the treatments with low density and high density of worms was not so evident (Figure S5). The presence of worm bioturbation resulted in the lower release of copper (Cont-NW < Cont-LD < Cont-HD) (Figure S5).

The time-weighted average concentrations of dissolved metals in the overlying water followed a similar trend (Table S5, Supporting Information). They were also uniformly lower than the corresponding water quality guideline values,[41] indicating the effectiveness of the water recirculation system in controlling the overlying water metal concentrations and suggesting exposure to this level of dissolved metals should not exert toxic effects to the chironomid worms.

Although the time-weighted average concentrations of dissolved metals and the metal assimilation rates for nickel and lead were determined in different compartments (in the overlying water and in the sediment) and over different time windows (dissolved metals on day 1 to day 20 and bioavailability on day 21), they were strongly correlated ($p < 0.001$ for Ni, $p = 0.002$ for Pb, Figure 5). These strong correlations suggested consistence between metal mobility and metal bioavailability near the SWI, with metals of higher mobility showing higher bioavailability.

3.5. Mobility, Bioavailability, and Toxicity of Ni within the Sediment−Water−Organism Nexus. Disturbances (physical or/and biological) to benthic sediments cause changes to metal mobility in benthic sediments.[42] The changes are understandable, but the effects of the changes on the toxicity risk of metals are not easily predicted.[1] Direct and simpler methods are desired that rapidly provide the information on metal bioavailability and reliably predict risks posed by exposing to bioavailable metals.

The toxicity response to the release of metals (into the overlying water, Figure S5, and to the porewater, Figures S7 and S8) in treatments with different sediments (clean vs contaminated sediments) suggested that the changing mobility of nickel was primarily responsible for the changes in observed sediment toxicity, as both the time-weighted average concentrations of dissolved nickel in the overlying water and that in the 1 cm porewater were also indicative of the observed sediment toxicity (Figures S9 and S10, Note S3, Table S6, Supporting Information).

Compared to relying on overlying water and/or porewater measurements, the isotopically modified bioassay provided a more accurate prediction of the toxicity risk (Table S6, lowest RMSE value—root mean square error—in the dose−toxicity

https://doi.org/10.1021/acs.est.2c06193
Environ. Sci. Technol. XXXX, XXX, XXX−XXX

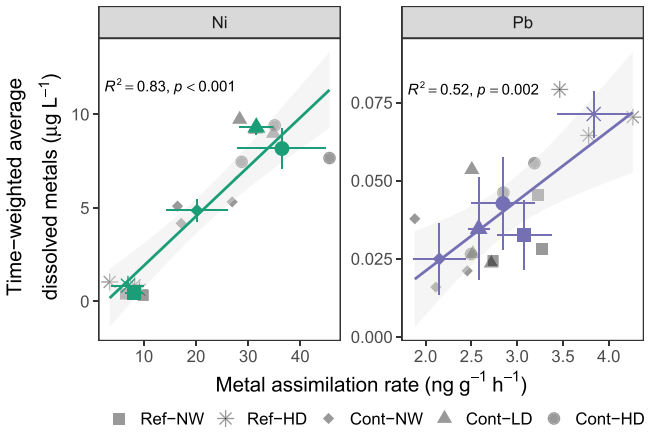

Figure 5. Strong correlations existed between the metal assimilation rate and time-weighted average dissolved metal concentrations. Each gray point represents the measurement in a replicate test; the colored points and the error bars represent the mean and standard deviation of the three replicate measurements for each of the five sediment treatments; the solid line is the linear regression line of the mean measurement, and the band is the 95% confidence band.

relationship regression using the nickel assimilation rate). An advantage of the isotopically modified bioassay is that it directly assesses the bioavailable metal exposure to an organism via both the aqueous exposure and through sediment ingestion. While the dissolved metal measurements provide the information on exposure to bioavailable metals through the aqueous pathway, the dietary contribution of sediment-bound bioavailable metals to the organisms cannot be neglected. Traditionally, this is often assessed separately based on equilibrium type models or from chemical-extraction measurement on subsamples of sediments.[43] Here, because the clams were exposed to a similar niche as the exposure environment of the chironomid worms, the bioassay directly measured metal bioavailability contributed by both sources as a whole and thus more accurately predict the toxicity risk (Figure 4).

The combination of the isotopically modified bioassay and dissolved metal measurements enabled further delineation of exposure pathways for bioavailable nickel within the sediment−water−biota nexus. This is done by assuming that the buried clams absorbed dissolved nickel from the 1 cm porewater at a known rate (that is similar to the uptake rate constant rate during the isotope-enriching stage) and then discriminate the dietary nickel assimilation as the difference between the total nickel assimilation rate and the aqueous nickel assimilation rate, as detailed in Note S4, Supporting Information.

The dietary nickel assimilation was estimated to contribute a major proportion of the total assimilation of nickel in the sedimentary system (ranging from 81 to 93% in different treatments, Table S7), suggesting that ingesting sediment was an important exposure pathway of nickel assimilation by the clams in the sediments. With increasing bioturbation intensities in the contaminated sediments, the dietary nickel assimilation rate also increased from 16 ng g^{-1} h^{-1} in the Cont-NW to 27 ng g^{-1} h^{-1} in the Cont-LD and to 29 ng g^{-1} h^{-1} in the Cont-HD (Table S7), suggesting that the bioturbation by tubificid worms can enhance the bioavailability of particulate nickel in sediments. Because in this study, the dissolved nickel concentrations in the overlying water and porewater and the densities of the tubificid worms were controlled at the level representative to those experienced within natural settings, the results clearly suggest that the role of dietary uptake of bioavailable nickel should not be ignored and the change in bioturbation intensity can alter the bioavailability of sediment-associated nickel enough to dictate the outcomes of sediment risk assessment.

3.6. Implications on Sediment Quality Risk Assessment. The bioavailability-based sediment quality risk assessment requires efficient and accurate measurement of contaminant bioavailability. In the present study, we developed an isotopically modified organism bioassay to simultaneously quantify the bioavailability of multiple metals in the bedded sediment. Because of the many merits of this approach, it can be readily adapted in different applications and for different species to improve both the scientific understanding of metal behavior in the sediment−water−biota nexus and the effectiveness of risk assessment for a more precise management of a contaminated site.

The behavior of metals in benthic sediments is subject to the coupled influence of different processes (e.g., hydrodynamics, geochemical cycling, and bioturbation).[44−47] Studies of metal behavior in sediments often simplify the real conditions by assuming that the sediment is equilibrated. However, the highly variable environmental conditions often result in changes in the physical, chemical, and biological conditions. While chemical measurements can usually be made within a relatively short period of time to capture the dynamic changes, most traditional biological measurements to determine the bioavailability and toxicity often require much longer time periods (weeks, months) and thus cannot provide information with enough temporal resolution. Because of the relatively higher sensitivity (compared with traditional long-term bioaccumulation approach), the isotopically modified organism bioassay only requires a short contaminant exposure time (24 h), which makes it feasible to capture the instantaneous changes in metal bioavailability in unequilibrated sediments. Therefore, the coupled effects of different benthic processes on the bioavailability and toxicity risk of metal contaminants can be evaluated with the assistance of this technique.

The merits of this new approach also make it suitable to be applied in different stages of a sediment quality risk assessment practice.[48] Because of the speed of the measurement, it may also be used at the initial screening stage with other chemical measurement (e.g., total metal concentration measurement) to rapidly diagnose the bioavailable contamination status of a site. Although this method has not been tested for direct field application, sediment cores or surficial sediments from the contaminated site can be collected and tested for metal bioavailability in laboratory-controlled conditions. In such cases, the isotopically modified organisms would not need to be acclimated to the variable field conditions and measurement uncertainties due to organisms' physiological maladaptation can be reduced. In later tiers of sediment quality assessments, when longer-term tests such as the sediment toxicity examinations are typically used, the isotopically modified organism bioassay can also be incorporated to provide insights on metal bioavailability in the test system. The use of multiple lines of evidence (chemical lability, toxicity, and bioavailability) to comprehensively assess the risk of contaminated sediments delivers a more reliable assessment outcome and thus benefits the execution of precise management.[48]

Overall, this study presented a new bioaccumulation-based approach to directly and rapidly quantify the bioavailability and

https://doi.org/10.1021/acs.est.2c06193
Environ. Sci. Technol. XXXX, XXX, XXX−XXX

toxicity risk of several metals simultaneously in benthic sediments. The approach can be readily adapted for multiple purposes, including the application in a sediment quality risk assessment practice. This study has also demonstrated that bioturbation by tubificid worms, at an intensity representative to those experience within the natural settings, can substantially change the mobility, bioavailability, and toxicity of metals in sediments. Therefore, natural disturbance processes such as bioturbation should be critically considered when developing conceptual site models in risk assessment and remediation designs.

■ ASSOCIATED CONTENT

Supporting Information

The Supporting Information is available free of charge at https://pubs.acs.org/doi/10.1021/acs.est.2c06193.

Details on the sampling and analysis, isotopic composition analysis, exposure-toxicity regression model, differentiation of nickel assimilation through different pathways, experimental setup, sediment characterization results, QA/QC results, release of dissolved metals in the overlying water, and temporal change of dissolved metals in porewater (PDF)

■ AUTHOR INFORMATION

Corresponding Author

Minwei Xie − *State Key Laboratory of Marine Environmental Science, Key laboratory of the Ministry of Education for Coastal and Wetland Ecosystem, College of the Environment and Ecology, Xiamen University, Xiamen, Fujian 361102, China;* orcid.org/0000-0003-4359-8738; Email: minweixie@xmu.edu.cn

Authors

Qiuling Wu − *State Key Laboratory of Marine Environmental Science, Key laboratory of the Ministry of Education for Coastal and Wetland Ecosystem, College of the Environment and Ecology, Xiamen University, Xiamen, Fujian 361102, China*

Qijing Su − *State Key Laboratory of Marine Environmental Science, Key laboratory of the Ministry of Education for Coastal and Wetland Ecosystem, College of the Environment and Ecology, Xiamen University, Xiamen, Fujian 361102, China*

Stuart L. Simpson − *Centre for Environmental Contaminants Research, CSIRO Land and Water, Lucas Heights, New South Wales 2232, Australia; Southern Marine Science and Engineering Guangdong Laboratory (Guangzhou), Guangzhou, Guangdong 511458, China*

Qiao-Guo Tan − *State Key Laboratory of Marine Environmental Science, Key laboratory of the Ministry of Education for Coastal and Wetland Ecosystem, College of the Environment and Ecology, Xiamen University, Xiamen, Fujian 361102, China;* orcid.org/0000-0001-9692-6622

Rong Chen − *State Key Laboratory of Marine Environmental Science, Key laboratory of the Ministry of Education for Coastal and Wetland Ecosystem, College of the Environment and Ecology, Xiamen University, Xiamen, Fujian 361102, China*

Complete contact information is available at: https://pubs.acs.org/10.1021/acs.est.2c06193

Notes

The authors declare no competing financial interest.

■ ACKNOWLEDGMENTS

We thank Dr. Huizhen Li from the Jinan University for providing us the chironomid larvae. We thank Dr. Graeme Batley and two anonymous reviewers for valuable comments to the manuscript. This study was supported by the National Natural Science Foundation of China (grant no.42077372), the Fundamental Research Funds for the Central Universities in China (grant no. 20720200113), and the Hong Kong Branch of Southern Marine Science and Engineering Guangdong Laboratory (Guangzhou) (grant no. SMSEGL20SC02).

■ REFERENCES

(1) Burton, G. A. Metal bioavailability and toxicity in sediments. *Crit. Rev. Environ. Sci. Technol.* **2010**, *40*, 852−907.

(2) Chapman, P. M.; Wang, F.; Janssen, C.; Persoone, G.; Allen, H. E. Ecotoxicology of metals in aquatic sediments: binding and release, bioavailability, risk assessment, and remediation. *Can. J. Fish. Aquat. Sci.* **1998**, *55*, 2221−2243.

(3) Burgess, R. M.; Berry, W. J.; Mount, D. R.; Di Toro, D. M. Mechanistic sediment quality guidelines based on contaminant bioavailability: Equilibrium partitioning sediment benchmarks. *Environ. Toxicol. Chem.* **2013**, *32*, 102−114.

(4) Rainbow, P. S. Trace metal bioaccumulation: models, metabolic availability and toxicity. *Environ. Int.* **2007**, *33*, 576−582.

(5) Xie, M.; Simpson, S. L.; Huang, J.; Teasdale, P. R.; Wang, W.-X. In Situ DGT sensing of bioavailable metal fluxes to improve toxicity predictions for sediments. *Environ. Sci. Technol.* **2021**, *55*, 7355−7364.

(6) Birch, G. A review of chemical-based sediment quality assessment methodologies for the marine environment. *Mar. Pollut. Bull.* **2018**, *133*, 218−232.

(7) Judd, N. L.; Toll, J. E.; McPeek, K.; Baldwin, A.; Bergquist, B.; Tobiason, K.; DeForest, D. K.; Santore, R. C. Collection and use of porewater data from sediment bioassay studies for understanding exposure to bioavailable metals. *Integr. Environ. Assess. Manage.* **2022**, *18*, 1321−1334.

(8) Hare, L. Aquatic insects and trace metals: bioavailability, bioaccumulation, and toxicity. *Crit. Rev. Toxicol.* **1992**, *22*, 327−369.

(9) ASTM International*Standard test method for measuring the toxicity of sediment-associated contaminants with freshwater invertebrates*; ASTM International: 2013.

(10) Simpson, S.; Campana, O.; Ho, K., Sediment toxicity testing. In *Marine ecotoxicology*; Elsevier: 2016; pp. 199−237, DOI: 10.1016/B978-0-12-803371-5.00007-2.

(11) Mann, R. M.; Hyne, R. V.; Simandjuntak, D. L.; Simpson, S. L. A rapid amphipod reproduction test for sediment quality assessment: in situ bioassays do not replicate laboratory bioassays. *Environ. Toxicol. Chem.* **2010**, *29*, 2566−2574.

(12) Costello, D. M.; Harrison, A. M.; Hammerschmidt, C. R.; Mendonca, R. M.; Burton, G. A., Jr. Hitting reset on sediment toxicity: sediment homogenization alters the toxicity of metal-amended sediments. *Environ. Toxicol. Chem.* **2019**, *38*, 1995−2007.

(13) Simpson, S. L.; Batley, G. E. Predicting metal toxicity in sediments: a critique of current approaches. *Integr. Environ. Assess. Manage.* **2007**, *3*, 18−31.

(14) Xie, M.; Jarrett, B. A.; Da Silva-Cadoux, C.; Fetters, K. J.; Burton, G. A., Jr.; Gaillard, J.-F.; Packman, A. I. Coupled effects of hydrodynamics and biogeochemistry on Zn mobility and speciation in highly contaminated sediments. *Environ. Sci. Technol.* **2015**, *49*, 5346−5353.

(15) Xie, M.; Alsina, M. A.; Yuen, J.; Packman, A. I.; Gaillard, J.-F. Effects of resuspension on the mobility and chemical speciation of zinc in contaminated sediments. *J. Hazard. Mater.* **2019**, *364*, 300−308.

(16) Amato, E. D.; Simpson, S. L.; Remaili, T. M.; Spadaro, D. A.; Jarolimek, C. V.; Jolley, D. F. Assessing the effects of bioturbation on metal bioavailability in contaminated sediments by diffusive gradients in thin films (DGT). *Environ. Sci. Technol.* **2016**, *50*, 3055−3064.
(17) Roche, K. R.; Aubeneau, A. F.; Xie, M.; Aquino, T.; Bolster, D.; Packman, A. I. An integrated experimental and modeling approach to predict sediment mixing from benthic burrowing behavior. *Environ. Sci. Technol.* **2016**, *50*, 10047−10054.
(18) Xie, M.; Wang, N.; Gaillard, J.-F.; Packman, A. I. Interplay between flow and bioturbation enhances metal efflux from low-permeability sediments. *J. Hazard. Mater.* **2018**, *341*, 304−312.
(19) Remaili, T. M.; Simpson, S. L.; Amato, E. D.; Spadaro, D. A.; Jarolimek, C. V.; Jolley, D. F. The impact of sediment bioturbation by secondary organisms on metal bioavailability, bioaccumulation and toxicity to target organisms in benthic bioassays: implications for sediment quality assessment. *Environ. Pollut.* **2016**, *208*, 590−599.
(20) Croteau, M. N.; Cain, D. J.; Fuller, C. C. Novel and nontraditional use of stable isotope tracers to study metal bioavailability from natural particles. *Environ. Sci. Technol.* **2013**, *47*, 3424−3431.
(21) Croteau, M. N.; Cain, D. J.; Fuller, C. C. Assessing the dietary bioavailability of metals associated with natural particles: extending the use of the reverse labeling approach to zinc. *Environ. Sci. Technol.* **2017**, *51*, 2803−2810.
(22) Wu, Q.; Zheng, T.; Simpson, S. L.; Tan, Q.-G.; Chen, R.; Xie, M. Application of a Multi-Metal Stable-Isotope-Enriched Bioassay to Assess Changes to Metal Bioavailability in Suspended Sediments. *Environ. Sci. Technol.* **2021**, *55*, 13005−13013.
(23) Smith, M. E.; Lazorchak, J. M.; Herrin, L. E.; Brewer-Swartz, S.; Thoeny, W. T. A reformulated, reconstituted water for testing the freshwater amphipod, *Hyalella azteca*. *Environ. Toxicol. Chem.* **1997**, *16*, 1229−1233.
(24) Xie, M.; Simpson, S. L.; Wang, W.-X. Bioturbation effects on metal release from contaminated sediments are metal-dependent. *Environ. Pollut.* **2019**, *250*, 87−96.
(25) Wu, Q.; Zhou, H.; Tam, N. F. Y.; Tian, Y.; Tan, Y.; Zhou, S.; Li, Q.; Chen, Y.; Leung, J. Y. S. Contamination, toxicity and speciation of heavy metals in an industrialized urban river: Implications for the dispersal of heavy metals. *Mar. Pollut. Bull.* **2016**, *104*, 153−161.
(26) Liu, W.; Guangyuan, L.; Wang, W.-X. *In situ* high-resolution two-dimensional profiles of redox sensitive metal mobility in sediment-water interface and porewater from estuarine sediments. *Sci. Total Environ.* **2022**, *820*, No. 153034.
(27) Simpson, S. L.; Pryor, I. D.; Mewburn, B. R.; Batley, G. E.; Jolley, D. Considerations for capping metal-contaminated sediments in dynamic estuarine environments. *Environ. Sci. Technol.* **2002**, *36*, 3772−3778.
(28) Vaughn, C. C.; Hakenkamp, C. C. The functional role of burrowing bivalves in freshwater ecosystems. *Freshwater Biol.* **2001**, *46*, 1431−1446.
(29) Doherty, F. G. The Asiatic clam, Corbicula spp., as a biological monitor in freshwater environments. *Environ. Monit. Assess.* **1990**, *15*, 143−181.
(30) Fisher, J. B.; Lick, W. J.; McCall, P. L.; Robbins, J. A. Vertical mixing of lake sediments by tubificid oligochaetes. *J. Geophys. Res.: Oceans* **1980**, *85*, 3997−4006.
(31) Gillis, P. L.; Diener, L. C.; Reynoldson, T. B.; Dixon, D. G. Cadmium-induced production of a metallothioneinlike protein in Tubifex tubifex (oligochaeta) and Chironomus riparius (diptera): Correlation with reproduction and growth. *Environ. Toxicol. Chem.* **2002**, *21*, 1836−1844.
(32) OECD*Sediment−water chironomid life-cycle toxicity test using spiked water or spiked sediment*; OECD: Paris, France., 2010.
(33) Bowles, K. C.; Apte, S. C.; Batley, G. E.; Hales, L. T.; Rogers, N. J. A rapid Chelex column method for the determination of metal speciation in natural waters. *Anal. Chim. Acta* **2006**, *558*, 237−245.
(34) Reible, D. D.; Popov, V.; Valsaraj, K. T.; Thibodeaux, L. J.; Lin, F.; Dikshit, M.; Todaro, M. A.; Fleeger, J. W. Contaminant fluxes from sediment due to tubificid oligochaete bioturbation. *Water Res.* **1996**, *30*, 704−714.
(35) Pelegri, S. P.; Blackburn, T. H. Effects of *Tubifex tubifex* (Oligochaeta: Tubificidae) on N-mineralization in freshwater sediments, measured with ^{15}N isotopes. *Aquat. Microb. Ecol.* **1995**, *9*, 289−294.
(36) Dumnicka, E. Composition and abundance of oligochaetes [Annelida: Oligochaeta] in springs of Krakow-Czestochowa Upland [Southern Poland]: effect of spring encasing and environmental factors. *Pol. J. Ecol.* **2006**, *54*, 231−242.
(37) Ma, P.; Li, H.; You, J. Full−Life Cycle Toxicity Assessment of Sediment-Bound DDT and Its Degradation Products on Chironomus dilutus. *Environ. Toxicol. Chem.* **2019**, *38*, 2698−2707.
(38) Li, H.; Sun, B.; Lydy, M. J.; You, J. Sediment-associated pesticides in an urban stream in Guangzhou, China: Implication of a shift in pesticide use patterns. *Environ. Toxicol. Chem.* **2013**, *32*, 1040−1047.
(39) Tan, Q.-G.; Lu, S.; Chen, R.; Peng, J. Making acute tests more ecologically relevant: cadmium bioaccumulation and toxicity in an estuarine clam under various salinities modeled in a toxicokinetic−toxicodynamic framework. *Environ. Sci. Technol.* **2019**, *53*, 2873−2880.
(40) Volpers, M.; Neumann, D. Tolerance of two tubificid species (Tubifex tubifex and Limnodrilus hoffmeisteri) to hypoxic and sulfidic conditions in novel, long-term experiments. *Arch. Hydrobiol.* **2005**, 13−38.
(41) ANZG, *Australian and New Zealand guidelines for fresh and marine water quality*. In Australian and New Zealand Governments and Australian State and Territory Governments: Canberra ACT, Australia, 2018.
(42) Eggleton, J.; Thomas, K. V. A review of factors affecting the release and bioavailability of contaminants during sediment disturbance events. *Environ. Int.* **2004**, *30*, 973−980.
(43) Lee, B.-G.; Griscom, S. B.; Lee, J.-S.; Choi, H. J.; Koh, C.-H.; Luoma, S. N.; Fisher, N. S. Influences of dietary uptake and reactive sulfides on metal bioavailability from aquatic sediments. *Science* **2000**, *287*, 282−284.
(44) Van Cappellen, P.; Gaillard, J.-F. Biogeochemical dynamics in aquatic sediments. *Rev. Mineral. Geochem.* **1996**, *34*, 335−376.
(45) Huettel, M.; Berg, P.; Kostka, J. E. Benthic exchange and biogeochemical cycling in permeable sediments. *Annu. Rev. Mar. Sci.* **2014**, *6*, 23−51.
(46) Huettel, M.; Røy, H.; Precht, E.; Ehrenhauss, S., Hydrodynamical impact on biogeochemical processes in aquatic sediments. In *The Interactions between Sediments and Water*; Springer: 2003; pp. 231−236, DOI: 10.1007/978-94-017-3366-3_31.
(47) Aller, R. C., Transport and reactions in the bioirrigated zone. In *The Benthic Boundary Layer: Transport Processes and Biogeochemistry*; Wiley2001; p 269.
(48) Simpson, S.; Batley, G., *Sediment quality assessment: a practical guide*; CSIRO Publishing: Melbourne, Victoria, Australia, 2016.

NOTE ADDED AFTER ASAP PUBLICATION

Originally published ASAP November 14, 2022; Equations 7 and 8 revised November 15, 2022.

https://doi.org/10.1021/acs.est.2c06193
Environ. Sci. Technol. XXXX, XXX, XXX−XXX

Isotopically-modified bioassay bridges the bioavailability and toxicity risk assessment of metals in bedded sediments

Supporting Information

Qiuling Wu[1], Qijing Su[1], Stuart L. Simpson[2,3], Qiao-Guo Tan[1], Rong Chen[1], Minwei Xie[1,*]

1. State Key Laboratory of Marine Environmental Science, Key laboratory of the Ministry of Education for Coastal and Wetland Ecosystem, College of the Environment and Ecology, Xiamen University, Xiamen, Fujian, 361102, China
2. Centre for Environmental Contaminants Research, CSIRO Land and Water, Lucas Heights, New South Wales 2232, Australia
3. Southern Marine Science and Engineering Guangdong Laboratory (Guangzhou), Guangzhou, Guangdong, 511458, China

*Corresponding Author: minweixie@xmu.edu.cn

This Supporting Information consists of 14 pages, including 10 figures and 7 tables.

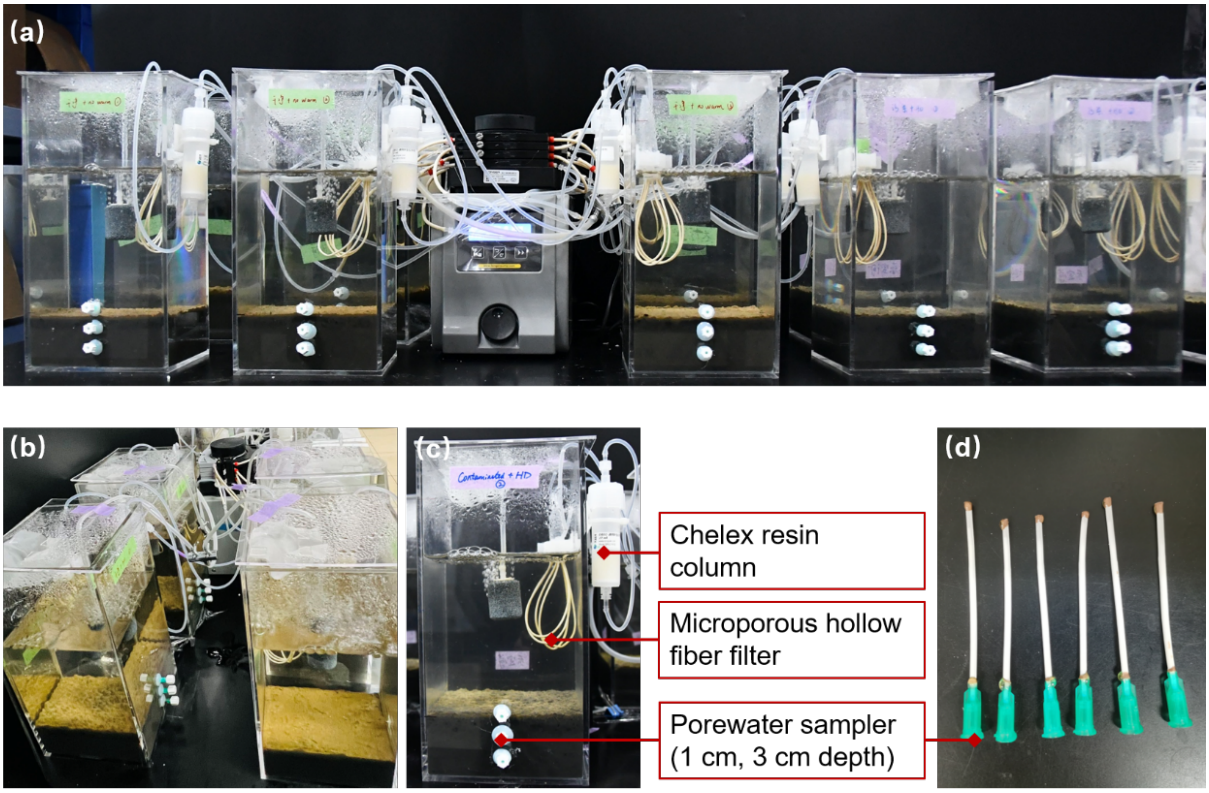

Figure S1. Experimental chamber. (a) Side view of the experimental setup. (b) Top view of the experimental setup. (c) components of the chamber: Chelex-resin column, microporous hollow-fiber filter and porewater sampler (only 1-cm and 3-cm depth ports were used). (d) Self-assembled microporous porewater sampler. The sampler consists of a piece of microporous hollow fiber (5 cm long, 2 mm in diameter, pore size of 0.15 μm) with one end sealed by epoxy resin while the other end attached to a plastic syringe needle adapter. When this sampler was deployed in the sediment, the porewater around the sampler was evenly extracted with the assistance of a vacuum generator (e.g. a syringe or a peristaltic pump).

S1. Sampling and analysis details.

Prior to the experiment, the sediments were characterized for total recoverable metal (TRM) concentrations. In brief, bulk homogenized sediments were freeze-dried (Model FD-1A-80, Biocool, Beijing), and then extracted in concentrated nitric acid at 180°C for 20 min in a microwave digestion system (Milestone ETHOS UP, Italy) following the USEPA Method 3051A.[1] Concurrently with the sediment sample extractions, a certified reference sediment (MESS-4 sediment, National Research Council Canada) were also subject to the same extraction procedure, and all acid extracts were diluted and analyzed by ICP-MS to determine TRM concentrations. Particle size distribution of the two sediments were also determined by

wet sieving the sediments successively through two sieves with a pore size of 150 and 75 µm, and determined the mass fraction of the sediments retained by each sieve (Table S1).

During the experiment, overlying water was monitored for dissolved oxygen (DO) concentrations and pH. The DO was measured using a DO probe (HQ30d, Hach) directly in the overlying water in each chamber and randomly on Day 0, 2, 10, and 21 to confirm it was oxygenated throughout the course of the experiment (DO = 8.8 ± 0.1 mg L^{-1}) . Five mL of overlying water was taken from each chamber to measure the pH (FE28-Standard, METTLER TOLEDO) at a two-day interval and the same volume of water was returned to the chamber after measurement. The overlying water was neutral to weakly basic (pH range of 7.5 to 8.0) throughout the test.

A series of quality control procedures were tested, including monitoring the concentration of internal reference standards (^{103}Rh, ^{74}Ge and ^{209}Bi, 5µg L^{-1}) to correct instrumental signal drift, measuring quality control standards (10 µg L^{-1} for all metals) for every 15-20 samples, and determining the metal concentrations in the certified reference materials (CRMs, oyster tissue and sediment). Recoveries were 96 to 105% for the CRM oyster tissue samples, and were 85 to 99% for the CRM sediment samples (Table S2).

Table S1. Total recoverable metal (TRM) concentrations in sediments

		Clean Sediment	Contaminated Sediment	SQGVs[†]
TRM (mg kg^{-1} dry weight)	Ni	6.3 ± 1.3	94 ± 1.8	21
	Cu	28 ± 7	480 ± 20	65
	Zn	180 ± 50	380 ± 10	200
	Cd	0.46 ± 0.14	0.77 ± 0.03	1.5
	Pb	110 ± 30	45 ± 5.4	50
	Mn	690 ± 20	370 ± 20	NV[‡]
	Fe	8700 ± 300	13000 ± 300	NV
Particle size distribution (Mass fraction)	>150 µm	35%	16%	NV
	75-150 µm	3%	10%	NV
	<75 µm	62%	74%	NV

[†] SQGVs = sediment quality guideline values.[2]

[‡] NV = no SQGV exists.

Table S2. Recoveries for certified reference materials (CRMs)

Metal	Recovery of CRM (%)	
	SRM-1996b oyster tissue (n = 3)	MESS-4 sediment (n = 3)
Ni	105 ± 3	89 ± 9
Cu	103 ± 3	89 ± 6
Cd	99 ± 2	97 ± 8
Pb	96 ± 3	85 ± 2
Zn	105 ± 5	99 ± 7

S2. Isotopic composition analysis

The aqueous uptake of metal stable isotopes during the isotope-enriching stage, the isotopic ratios (labeled : unlabeled isotopes) in the clam tissue, and the metal assimilation rate from the sediments (i.e. metal bioavailability) can be quantified by tracking the isotopic composition in the clams at the end of different stages. For brevity, the percentile numbers appeared in the following equations represent the natural abundance of the metal stable isotope (Table S3). The meaning of the symbols was explained in the manuscript (Section 2.8).

(1) Aqueous uptake of ^{62}Ni, ^{112}Cd, ^{114}Cd, ^{206}Pb, and ^{65}Cu were calculated in Equation S1 to S5 (refer to Figure S2 for the derivation of $[^{61}\mathrm{Ni}]_{\mathrm{new}}$ as an example).

$$[^{62}\mathrm{Ni}]_{\mathrm{new}} = [^{62}\mathrm{Ni}]_{\mathrm{meas}} \times 3.63\% - [^{60}\mathrm{Ni}]_{\mathrm{meas}} \times 3.63\% \quad \text{(S1)}$$

$$[^{112}\mathrm{Cd}]_{\mathrm{new}} = [^{112}\mathrm{Cd}]_{\mathrm{meas}} \times 24.1\% - [^{111}\mathrm{Cd}]_{\mathrm{meas}} \times 24.1\% \quad \text{(S2)}$$

$$[^{114}\mathrm{Cd}]_{\mathrm{new}} = [^{114}\mathrm{Cd}]_{\mathrm{meas}} \times 28.7\% - [^{111}\mathrm{Cd}]_{\mathrm{meas}} \times 28.7\% \quad \text{(S3)}$$

$$[^{206}\mathrm{Pb}]_{\mathrm{new}} = [^{206}\mathrm{Pb}]_{\mathrm{meas}} \times 24.1\% - [^{207}\mathrm{Pb}]_{\mathrm{meas}} \times 24.1\% \quad \text{(S4)}$$

$$[^{65}\mathrm{Cu}]_{\mathrm{new}} = [^{65}\mathrm{Cu}]_{\mathrm{meas}} \times 30.8\% - [^{63}\mathrm{Cu}]_{\mathrm{meas}} \times 30.8\% \quad \text{(S5)}$$

(2) The isotopic ratio between the labeled and unlabeled isotope for $\mathrm{Ni}^{62/60}$, $\mathrm{Cd}^{112/111}$, $\mathrm{Cd}^{114/111}$, $\mathrm{Pb}^{206/207}$, and $\mathrm{Cu}^{65/63}$ were calculated in Equation S6 to S10.

$$\mathrm{Ni}^{62/60} = \frac{[^{62}\mathrm{Ni}]_{\mathrm{meas}} \times 3.63\%}{[^{60}\mathrm{Ni}]_{\mathrm{meas}} \times 26.2\%} \quad \text{(S6)}$$

$$\mathrm{Cd}^{112/111} = \frac{[^{112}\mathrm{Cd}]_{\mathrm{meas}} \times 24.1\%}{[^{111}\mathrm{Cd}]_{\mathrm{meas}} \times 12.8\%} \quad \text{(S7)}$$

$$\mathrm{Cd}^{114/111} = \frac{[^{114}\mathrm{Cd}]_{\mathrm{meas}} \times 28.7\%}{[^{111}\mathrm{Cd}]_{\mathrm{meas}} \times 12.8\%} \quad \text{(S8)}$$

$$\mathrm{Pb}^{206/207} = \frac{[^{206}\mathrm{Pb}]_{\mathrm{meas}} \times 24.1\%}{[^{207}\mathrm{Pb}]_{\mathrm{meas}} \times 22.1\%} \quad \text{(S9)}$$

$$\mathrm{Cu}^{65/63} = \frac{[^{65}\mathrm{Cu}]_{\mathrm{meas}} \times 30.85\%}{[^{63}\mathrm{Cu}]_{\mathrm{meas}} \times 69.15\%} \quad \text{(S10)}$$

(3) The assimilation rate of Ni (calculated from the change of $^{62/60}$Ni) and that of Pb were calculated using the equation S11 to S15.

$$\mathrm{Ni}^{62/60}|_{\mathrm{base}} = \frac{W \times [^{62}\mathrm{Ni}]_{\mathrm{meas|exp}} \times 3.63\% - M_{\mathrm{Ni}} \cdot 3.63\%}{W \times [^{60}\mathrm{Ni}]_{\mathrm{meas|exp}} \times 26.2\% - M_{\mathrm{Ni}} \cdot 26.2\%} \quad \text{(S11)}$$

$$\mathrm{Pb}^{206/207}|_{\mathrm{base}} = \frac{W \times [^{206}\mathrm{Pb}]_{\mathrm{meas|exp}} \times 24.1\% - M_{\mathrm{Pb}} \cdot 24.1\%}{W \times [^{207}\mathrm{Pb}]_{\mathrm{meas|exp}} \times 22.1\% - M_{\mathrm{Pb}} \cdot 22.1\%} \quad \text{(S12)}$$

$$M_{\mathrm{Ni}} = \frac{W \times \left(\mathrm{Ni}^{62/60}|_{\mathrm{base}} \times [^{60}\mathrm{Ni}]_{\mathrm{meas|exp}} \times 26.2\% - [^{62}\mathrm{Ni}]_{\mathrm{meas|exp}} \times 3.63\% \right)}{\mathrm{Ni}^{62/60}|_{\mathrm{base}} \times 26.2\% - 3.63\%} \quad \text{(S13)}$$

$$M_{\mathrm{Pb}} = \frac{W \times (\mathrm{Pb}^{206/207}|_{\mathrm{base}} \times [^{207}\mathrm{Pb}]_{\mathrm{meas|exp}} \times 22.1\% - [^{206}\mathrm{Pb}]_{\mathrm{meas|exp}} \times 24.1\%)}{\mathrm{Pb}^{206/207}|_{\mathrm{base}} \times 22.1\% - 24.1\%} \quad \text{(S14)}$$

$$\text{Assimilation rate} = \frac{M}{W \times t_{\mathrm{exp}}} \quad \text{(S15)}$$

Table S3. Metal stable isotopes used in this study and their natural abundance

Metal	Symbol	% Abundance
Nickel	^{61}Ni	1.14
	^{62}Ni	3.63
	^{60}Ni	26.2
Cadmium	^{112}Cd	24.1
	^{114}Cd	28.7
	^{111}Cd	12.8
Lead	^{206}Pb	24.1
	^{207}Pb	22.1
Copper	^{65}Cu	30.8
	^{63}Cu	69.2

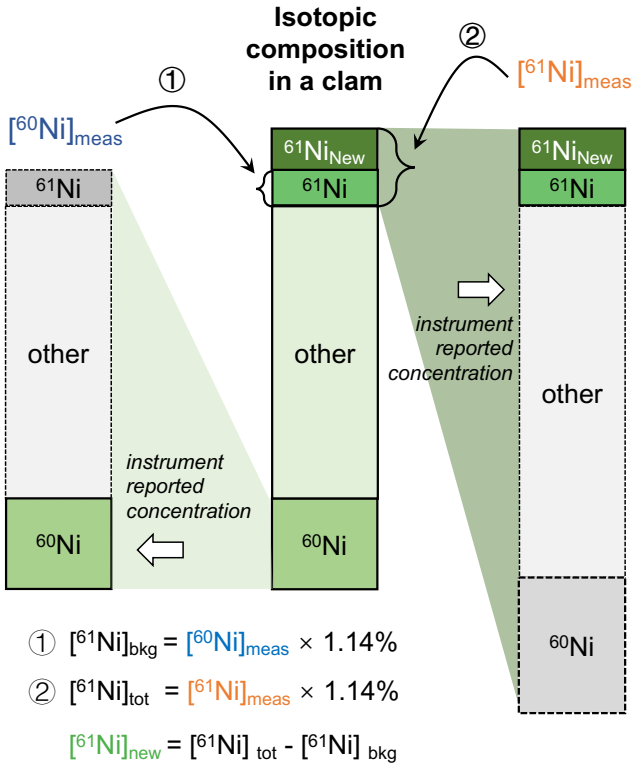

Figure S2. A sketch showing the derivation of newly accumulated nickel isotope ^{61}Ni from the measured concentrations of different nickel isotopes in one organism reported by the ICP-MS. The number 1.14% is the natural abundance of ^{61}Ni.

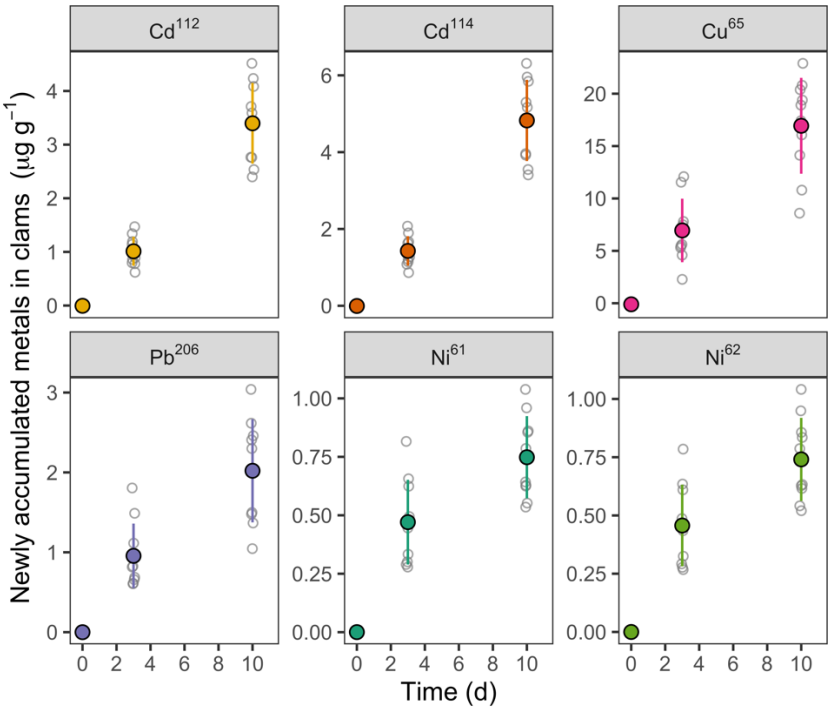

Figure S3. Concentrations of the newly accumulated Ni^{61}, Ni^{62}, Pb^{206}, Cd^{112}, Cd^{114}, and Cu^{65} in the clam tissue during the 10-d isotope-enriching stage. The spiked metal concentration in water were 5 μg L^{-1} for Ni^{61}, Ni^{62} and Pb^{206}, 2 μg L^{-1} for Cd^{112}, 3 μg L^{-1} for Cd^{114}, and 10 μg L^{-1} for Cu^{65}. Each open circle represents the concentration of the newly accumulated isotope in the tissue of an individual clam, the solid points represent the mean while the error bar represents the standard deviation.

Table S4. The background metal concentrations in the clam tissue (n =10)

Metal	Background concentrations ($\mu g\ g^{-1}$ dry weight)
Ni	0.31 ± 0.12
Cu	30 ± 8
Cd	0.94 ± 0.13
Pb	0.11 ± 0.03

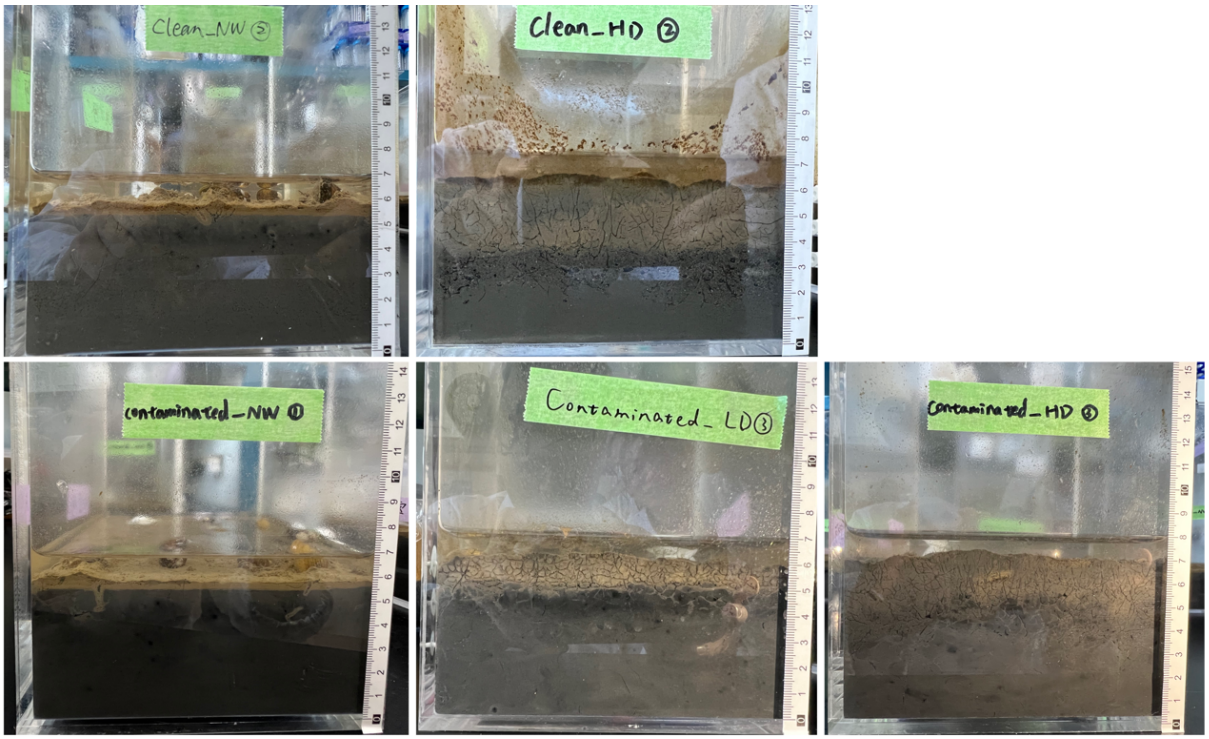

Figure S4. Bioturbation by the tubificid worms altered the physical and chemical structure of surficial sediments. Side view photos of the experiment chambers were taken before the addition of the isotopically-modified clams on Day 20 (with overlying water drained to 1 cm depth). Top two from left to right: the clean sediment without tubificid worms (Ref-NW), the clean sediment with high-density of worms (Ref-HD); Bottom three from left to right: Contaminated sediment with no worms (Cont-NW); Contaminated sediment with low-density of worms (Cont-LD); Contaminated sediment with high-density of worms (Cont-HD).

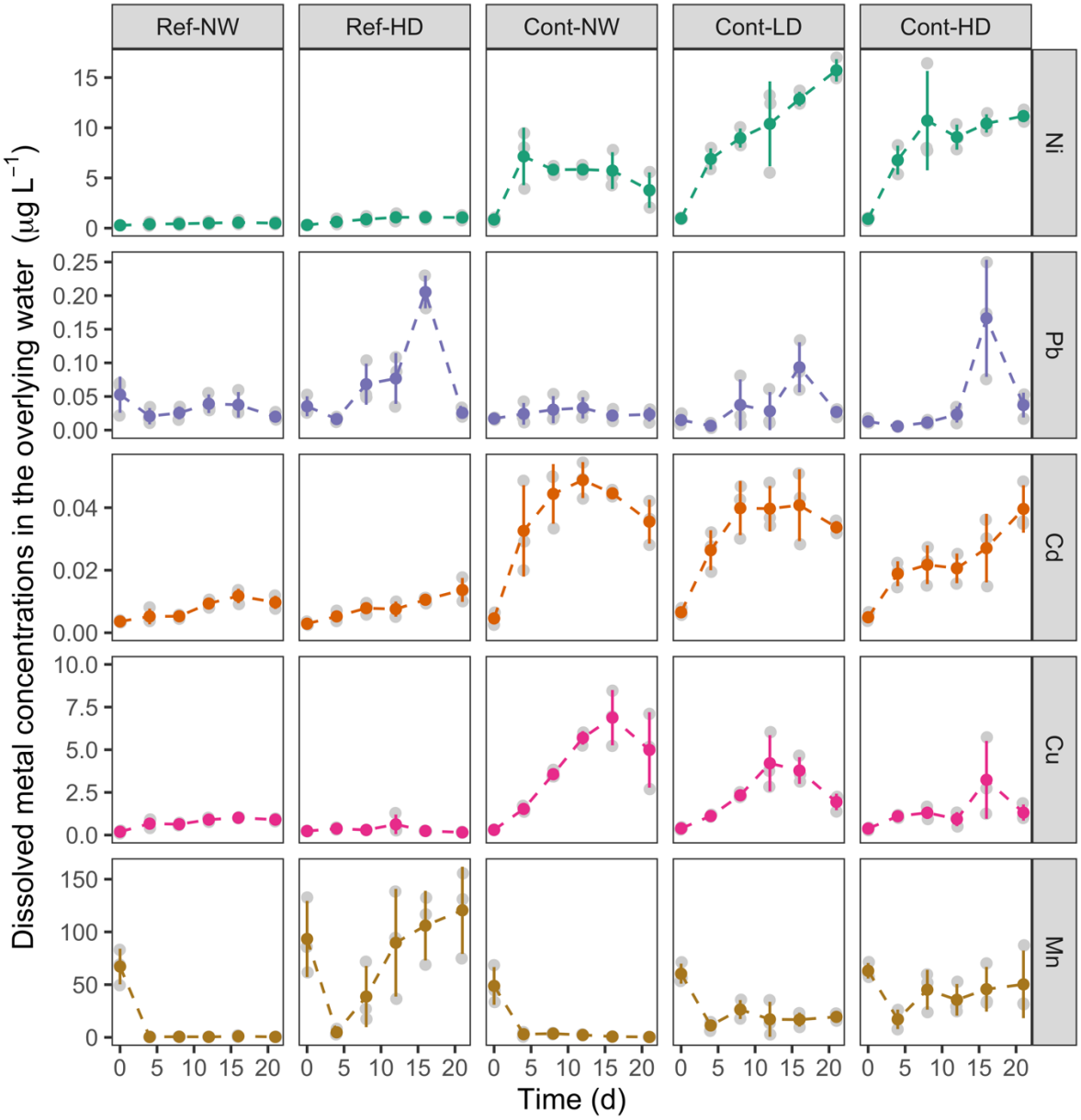

Figure S5. Dissolved metal concentrations in overlying water during 22-d toxicity testing.

Table S5. Time-weighted average metal concentrations in overlying water over the first 20 days

	Time-weighted average dissolved metal concentrations (µg L^{-1})					WQGVs† (µg L^{-1})
	Ref-NW	Ref-HD	Cont-NW	Cont-LD	Cont-HD	
Ni	0.44 ± 0.10	0.84 ± 0.20	1.2 ± 0.0	9.3 ± 0.4	8.2 ± 1.0	11
Pb	0.03 ±0.01	0.07 ± 0.007	0.05 ± 0.03	0.03 ± 0.02	0.04 ± 0.01	3.4
Cd	0.0070 ± 0.0008	0.0080 ± 0.0008	0.04 ± 0.01	0.03 ±0.01	0.02 ± 0.00	0.2
Cu	0.7 ± 0.1	0.3 ± 0.1	3.8 ± 0.3	2.3 ± 0.5	1.4 ± 0.5	1.4

† WQGVs = Water quality guideline values.[3]

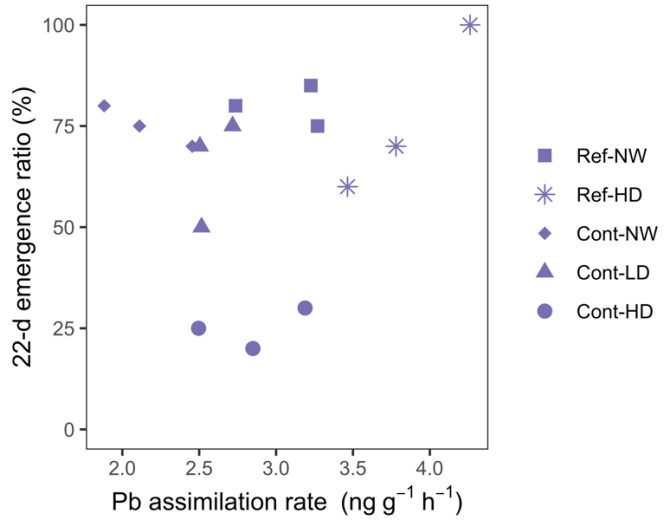

Figure S6. The Pb assimilation rate did not explain toxicity to the chironomids. Each point represents the measurement in a replicate test.

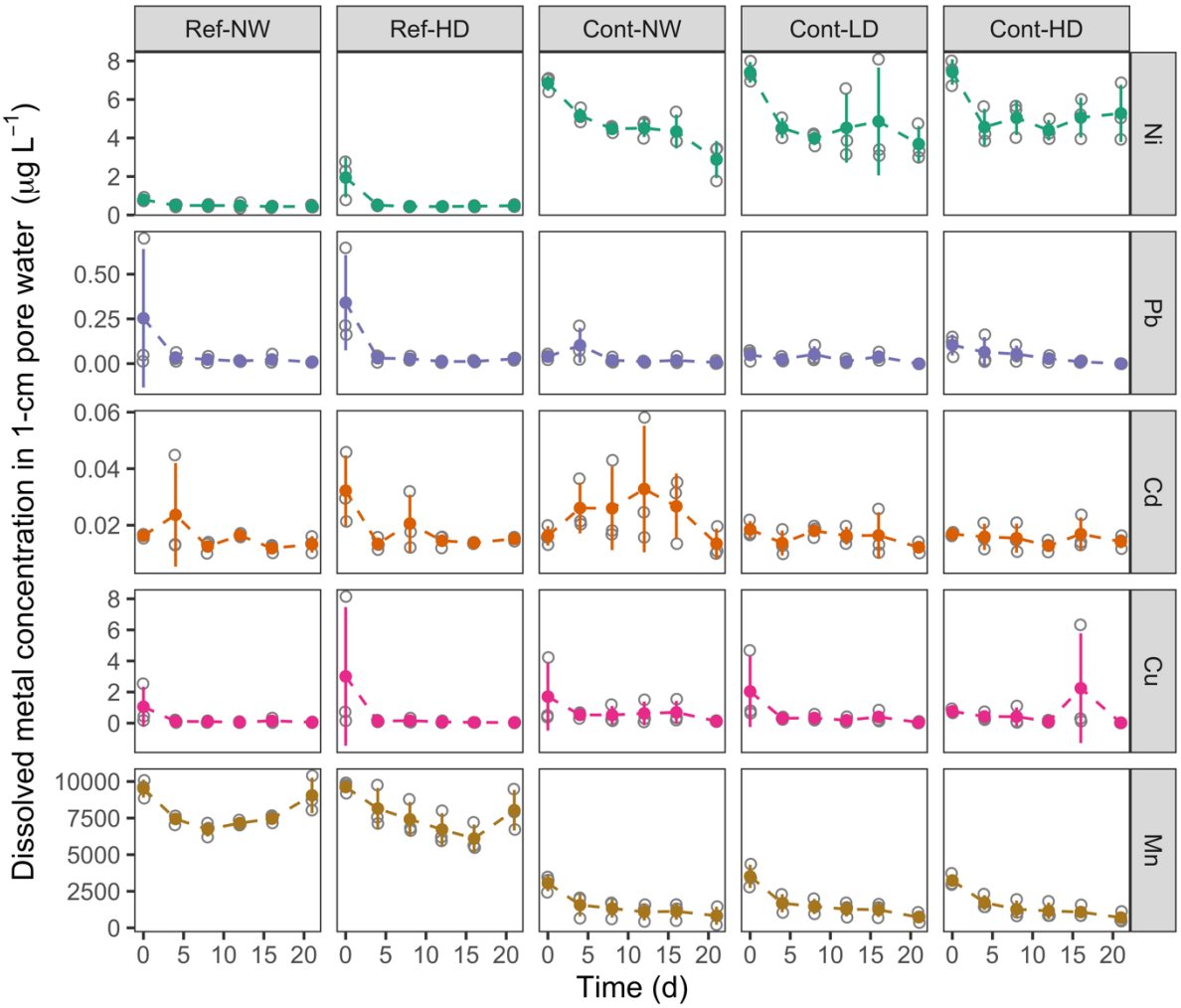

Figure S7. Metal concentrations in 1-cm porewater during the 22-d toxicity testing.

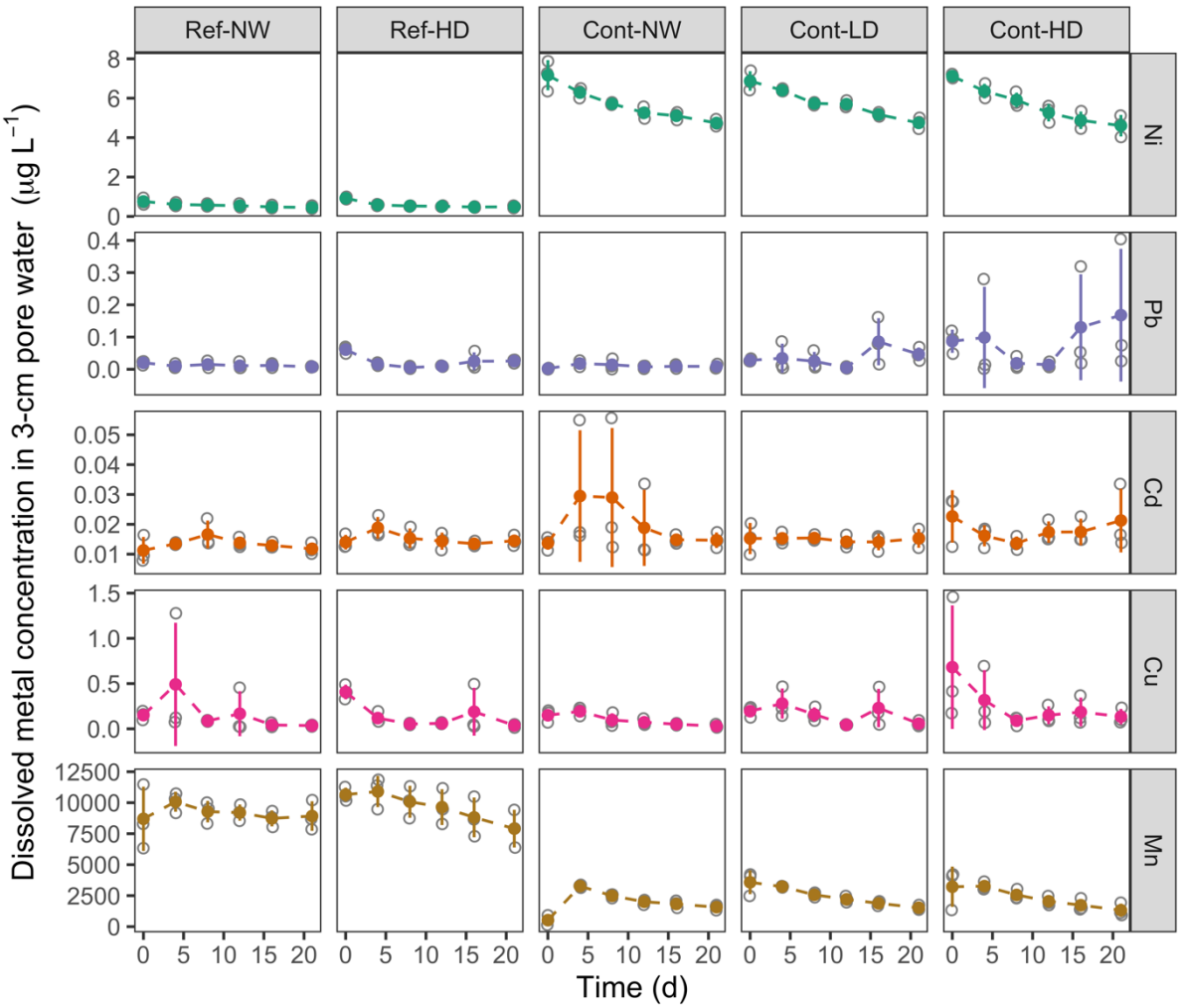

Figure S8. Metal concentration in 3-cm porewater during the 22-d toxicity testing.

S3. Regression with a logistic model

To quantitatively assess the dose-response relationship between nickel exposure and sediment toxicity, we employed a logistic model to fit the data.

$$\text{Emergence} = \frac{100}{1+e^{(\beta_0-\beta_1\times Ni_{\text{exp}})}} \quad \text{(S14)}$$

where Emergence is the 22-d emergence ratio (%), β_0 is the intercept parameter, and β_1 is the slope parameter. Ni_{exp} represents the exposure "concentration" of nickel when different dose-response relationship is evaluated, and thus this "concentration" corresponds to the nickel assimilation rate, the time-weighted average dissolved metal concentration in the

overlying water, and the time-weighted average dissolved metal concentration in the 1-cm porewater, respectively.

The regression was applied to the results obtained from the 15 individual replicate experiments. The data for each of the three "concentrations" were modeled independently. The data was fitted using the least-squares estimation method by the *nls( )* function in R (version 3.6.3). The performance of the regression fitting between each model were assessed by comparing the parameter root mean square error (RMSE, i.e., the standard deviation of the residuals), with smaller RMSE value indicating better fitting performance. In the logistic model, the slope parameter β_1 describes how the toxic effect respond to changing exposure concentrations.[4, 5] Here, the probability (p value) associated with β_1 was 0.0045 for the dataset with Ni assimilation rate, 0.033 for the dataset with the OW-nickel, and 0.02 for the dataset with the PW-nickel (Table S6), suggesting the toxic effect respond to the varying exposure "concentrations" at different significant levels. Therefore, the null hypothesis (slope $\beta_1 = 0$, toxicity does not respond to varying exposure "concentrations") can be rejected. The RMSE value was the lowest when the Ni assimilation rate was used to predict the toxicity (Table S6), suggesting that prediction with the Ni assimilation rate determined by the isotopically-modified bioassay was the most accurate among the three.

Table S6. Parameters of the regression using a logistic model

Modeling dataset	Intercept parameter β_0 (p)	Slope parameter β_1 (p)	RMSE
Ni assimilation rate	-1.91 (p = 0.0016)	-0.06 (p = 0.0045)	16.0
OW-nickel	-1.41 (p = 0.010)	-0.16 (p = 0.033)	19.5
PW-nickel	-1.69 (p = 0.011)	-0.31 (p = 0.028)	18.9

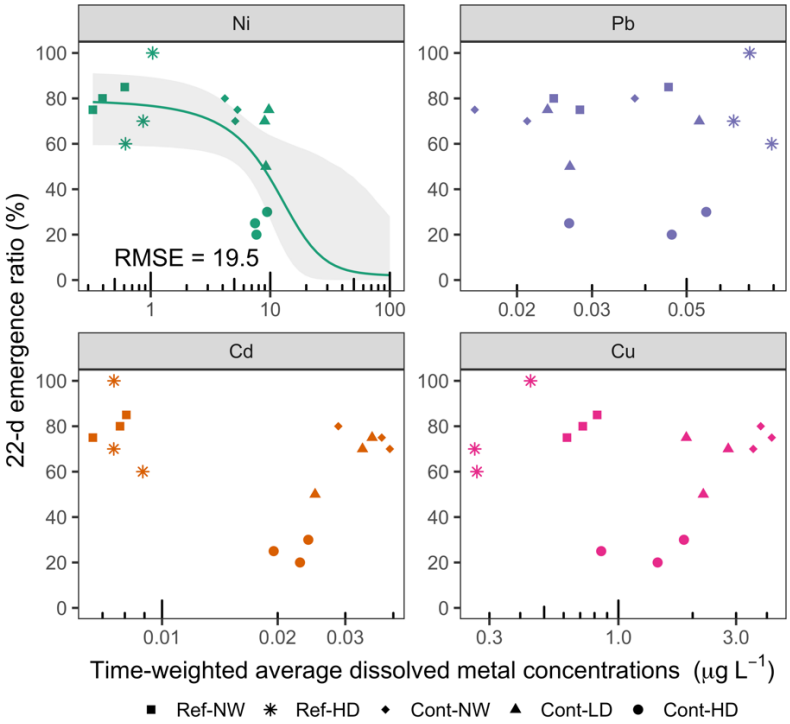

Figure S9. Relationship between 22-d emergence ratio and time-weighted average dissolved metal concentrations in overlying water. Each point represents the measurement in a replicate test. The solid line is the regression line of the measurement using the logistic model and the band is the 95% confidence band. RMSE stands for the root mean square error of the regression.

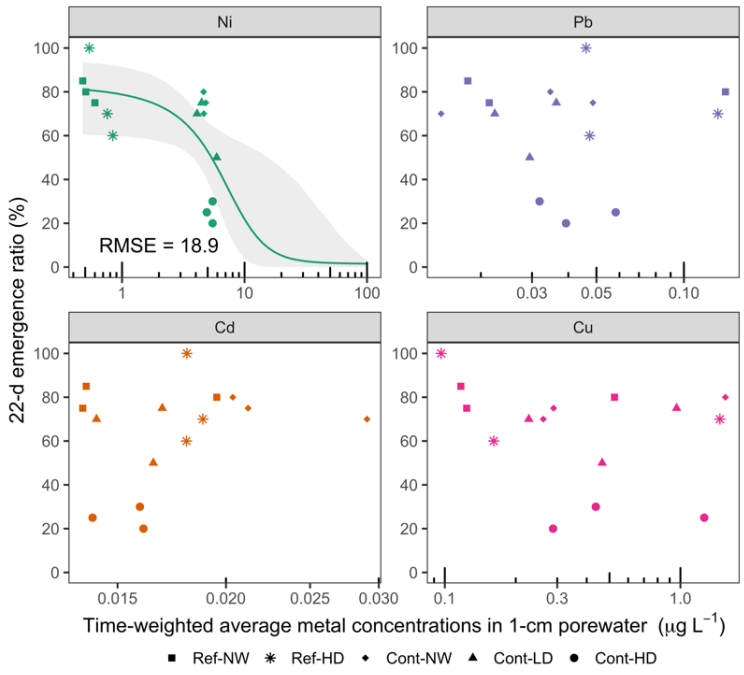

Figure S10. Relationship between 22-d emergence ratio and time-weighted average dissolved metal concentrations in 1-cm porewater. Each point represents the measurement in a replicate test. The solid line is the regression line of the measurement using the logistic model and the band is the 95% confidence band. RMSE stands for the root mean square error of the regression.

S4. Calculation of nickel assimilation through different pathway

The combination of the isotopically-modified bioassay and dissolved metal measurements enabled further delineation of exposure pathways for bioavailable nickel within the sediment-water-biota nexus (Table S7).

Because the clams were shallowly buried in the sediments and the overlying water was renewed with clean water before the addition of the clams, we assumed the primary aqueous exposure pathway of nickel assimilation was via exposing to the 1-cm porewater. The nickel accumulation via the porewater exposure (unit: $\mu g\ g^{-1}$) was then roughly estimated by multiplying the 24-h of exposure time with the porewater nickel concentration and the apparent aqueous nickel accumulation rate constant (unit: $L\ g^{-1}\ h^{-1}$) during the isotope-enriching phase (assuming the net accumulation rate in the porewater and in the reconstituted freshwater are the same), which was calculated by normalizing the increasing rate of the newly accumulated Ni^{61} concentrations *over the first 3 days* (Figure S3) with the Ni^{61} concentration in the aqueous solution.

The total nickel assimilation ($ng\ g^{-1}\ h^{-1}$) was calculated by multiplying the Ni assimilation rate (determined by the isotopically-modified bioassay, unit: $ng\ g^{-1}\ h^{-1}$, Figure 2 in the main text) with the 24-h exposure time.

The dietary nickel uptake was then calculated by subtracting the aqueous nickel uptake from the total nickel assimilation, and then converting to the dietary Ni uptake rate (unit: $ng\ g^{-1}\ h^{-1}$). The dietary nickel uptake rate followed similar trends as the total nickel assimilation rate in the sediments. It was higher in the contaminated sediment relative to that in the clean sediments. In the treatment with contaminated sediments, it increased with increasing density of the tubificid worms.

The dietary nickel uptake contribution can also be determined by dividing the dietary uptake rate by the total nickel assimilation rate. The dietary nickel uptake contribution ranged from 81% to 93%, suggesting the contribution was derived by dividing the dietary nickel uptake by the total nickel assimilation, and expressed in percentile (Table S7).

Table S7. Contribution of Ni assimilation by clams through different pathway

		Ref-NW	Ref-HD	Cont-NW	Cont-LD	Cont-HD
Aqueous Ni uptake rate constant (L g^{-1} h^{-1})				0.0013		
Dissolved Ni concentration in 1-cm porewater (µg L^{-1})		0.45	0.48	2.9	3.7	5.3
Ni accumulation from porewater (µg g^{-1})		0.014	0.015	0.090	0.12	0.17
Total Ni assimilation in sediments	Ni assimilation rate (ng g^{-1} h^{-1})	8.1	6.9	20	32	36
	Total Ni assimilation $[Ni]_{tot}$ (µg g^{-1})	0.19	0.17	0.48	0.77	0.86
Dietary Ni uptake (µg g^{-1})		**0.18**	**0.15**	**0.39**	**0.65**	**0.70**
Dietary Ni uptake rate (ng g^{-1} h^{-1})		**7.5**	**6.3**	**16**	**27**	**29**
Dietary Ni uptake contribution (%)		93%	90%	81%	85%	81%

REFERENCE

1. Element, C. A. S., Method 3051A. Microwave assisted acid digestion of sediments, sludges, soils, and oils. **2007**.

2. Simpson, S.; Batley, G., *Sediment quality assessment: a practical guide*. CSIRO Publishing: Melbourne, Victoria, Australia, 2016.

3. ANZG, Australian and New Zealand guidelines for fresh and marine water quality. In Australian and New Zealand Governments and Australian State and Territory Governments. Canberra ACT, Australia, 2018.

4. Field, L. J.; MacDonald, D. D.; Norton, S. B.; Severn, C. G.; Ingersoll, C. G., Evaluating sediment chemistry and toxicity data using logistic regression modeling. *Environmental Toxicology and Chemistry* **1999,** *18*, (6), 1311-1322.

5. Field, L. J.; MacDonald, D. D.; Norton, S. B.; Ingersoll, C. G.; Severn, C. G.; Smorong, D.; Lindskoog, R., Predicting amphipod toxicity from sediment chemistry using logistic regression models. *Environmental Toxicology and Chemistry* **2002,** *21*, (9), 1993-2005.